

Accepted Manuscript

Tectonic and depositional setting of the lower Cambrian and lower Silurian marine shales in the Yangtze Platform: Implications for Shale Gas Exploration and Production

Zhengyu Xu, Shu Jiang, Genshun Yao, Xing Liang, Shaoyun Xiong

PII: S1367-9120(18)30447-4

DOI: <https://doi.org/10.1016/j.jseaes.2018.10.023>

Reference: JAES 3684

To appear in: *Journal of Asian Earth Sciences*

Received Date: 1 February 2017

Revised Date: 21 October 2018

Accepted Date: 28 October 2018

Please cite this article as: Xu, Z., Jiang, S., Yao, G., Liang, X., Xiong, S., Tectonic and depositional setting of the lower Cambrian and lower Silurian marine shales in the Yangtze Platform: Implications for Shale Gas Exploration and Production, *Journal of Asian Earth Sciences* (2018), doi: <https://doi.org/10.1016/j.jseaes.2018.10.023>

This is a PDF file of an unedited manuscript that has been accepted for publication. As a service to our customers we are providing this early version of the manuscript. The manuscript will undergo copyediting, typesetting, and review of the resulting proof before it is published in its final form. Please note that during the production process errors may be discovered which could affect the content, and all legal disclaimers that apply to the journal pertain.



**Tectonic and depositional setting of the
lower Cambrian and lower Silurian marine shales in the
Yangtze Platform:
Implications for Shale Gas Exploration and Production**

Zhengyu Xu^a, Shu Jiang^{b,c,d*}, Genshun Yao^a,

Xing Liang^e, Shaoyun Xiong^a

^a PetroChina Hangzhou Institute of Geology, Hangzhou, China

^b Key Laboratory of Tectonics and Petroleum Resources of Ministry of Education,
China University of Geosciences, Wuhan, China

^c Energy and Geoscience Institute, University of Utah, Salt Lake City, Utah, USA

^d Research Institute of Unconventional Oil & Gas and Renewable Energy, China
University of Petroleum (East China), China

^e PetroChina Zhejiang Oilfield Company, Hangzhou, China

* Corresponding author.

E-mail address: sjiang@egi.utah.edu (S. Jiang).

ABSTRACT

Marine shales of the Lower Cambrian Qiongzhusi and Lower Silurian Longmaxi formations are extensively distributed in the Yangtze Platform. Detailed depositional and tectonic analyses and regional mapping indicated that the organic-rich Qiongzhusi-equivalent shale was deposited in an intra-shelf low-slope environment in a passive margin setting. The

Longmaxi-equivalent shale was mainly deposited in a widely-distributed intra-shelf low setting in the Upper and Middle Yangtze, and in a distal foredeep area away from clastic dilution in the Lower Yangtze Platform. The transgressive and early highstand system tracts in both Qiongzhusi and Longmaxi shales produced the best-quality shale reservoirs, with high total organic matter (TOC) content (>2%) and high quartz content (>45%). Tectonics has substantial effects on coeval deposition of organic-rich shale and its hydrocarbon accumulation and production. Later tectonism deformed the shales and disrupted early shale gas accumulation. Recent shale gas resource exploration and geologic analysis suggested that the high rate of shale gas production is due to overpressured marine shale reservoirs with high TOC and high gas content in the tectonically-stable area. Shale gas production occurred at reduced rates in slightly underpressured shale reservoirs with lower gas content in the syncline of the tectonically-transitional area deformed by three tectonic movements. There was no gas production from shales in the tectonically-active area disrupted by at least four tectonic movements and complex faults. The results of this analysis indicate that local tectonically-stable areas in the Middle and Lower Yangtze platforms may have shale gas accumulation and production potential.

Keywords: Tectonics, Depositional setting, Yangtze Platform, Marine shale, Shale gas resource

1. Introduction

Advances in hydraulic fracturing, horizontal drilling, geological characterization, and characterization of shale properties have greatly expanded shale gas production in the United States, and have revolutionized the US energy market (Curtis, 2002; Steward, 2007; EIA, 2013). In China, shale gas exploration is only just beginning. In 2013, commercially-viable shale gas was produced from the Lower Silurian Longmaxi marine shale in the Fuling Shale Gas Field in the southeast Sichuan Basin, making China the only country outside North America that has reported commercial production (Jiang, 2014). Resource assessment, exploration activities and preliminary production indicate that the Lower Paleozoic marine shales distributed throughout the Yangtze Platform hold the most shale gas reserves (Zhang *et al.*, 2008; Zou *et al.*, 2010; Zhang *et al.*, 2012; Du *et al.*, 2015; Jiang *et al.*, 2015, 2016). Exploration and analyses indicated promising results were mainly from individual pockets in the Sichuan Basin and adjacent areas in the Upper Yangtze Platform located to the west of Huangling anticline in Hubei Province. There was virtually no evidence for shale gas production in the Lower Yangtze Platform (located to the east and southeast of Tanlu Fault), and results indicated limited production in the Middle Yangtze Platform located between Upper and Lower Yangtze Platforms (Tan *et al.*, 2014; Jiang *et al.*, 2015, 2016) (Fig. 1). The production capabilities varied widely, even for adjacent producing shale reservoirs with the same geochemical properties and depositional facies.

Compared to successful North American marine shales, the complex geology of the Yangtze Platform presents many challenges, which previous analyses suggest are primarily due to active tectonic movement resulting in large deformations in the organic-rich shale, as well as the possible loss of the accumulated shale gas (Hao *et al.*, 2013 and Ju *et al.*, 2014). However, these studies lacked both an integrated depositional-tectonic analysis of shale reservoirs for multiple sites and the support of industry data regarding production rates for different depositional and tectonic conditions.

Many studies have focused on source rock potentials for conventional hydrocarbon accumulations, depositional environments, and regional distribution of the Lower Paleozoic shales (Lu, 1979; Su *et al.*, 2002; Feng *et al.*, 2004; Ma *et al.*, 2004; Zhang *et al.*, 2008; Zou *et al.*, 2010; Liu *et al.*, 2013; Tan *et al.*, 2014, Wu *et al.*, 2014). The depositional models and facies terminology from these previous studies were not widely adapted due to a lack of consistent nomenclature usage across the Yangtze Platform. Additionally, these publications only addressed the basic regional distribution of Lower Paleozoic Cambrian or Silurian shales, based on previous data for the Lower Cambrian and Lower Silurian (for example, thick gross interval or limited sample-specific measurements for local shales, and single-well analysis). Furthermore, comprehensive studies are lacking for shale deposition and tectonics across the Yangtze Platform. Systematic analyses of controlling factors on regional shale distribution, reservoir properties, and the relationship

between shale properties and shale gas accumulation and production are necessary to further elucidate Yangtze Platform production potential. The gaps between regional-scale geology and shale properties and fine-scale shale reservoir properties and production performance have yet to be bridged.

This paper investigates (1) the distribution and stratigraphic correlation of Lower Paleozoic (Cambrian and Ordovician to Silurian) marine shales, and (2) the temporal and spatial variation of geochemical, mineralogical, petrographic, and facies properties in shale over a range of tectonic settings. This paper also seeks to elucidate how depositional facies and structural activities influence shale reservoir quality, shale gas accumulation, and preservation and production. These analyses will help relate complex depositional and tectonic variations to shale reservoir development, shale gas exploration, and production for the Paleozoic marine shales in the Yangtze Platform, and provides baseline data for other shales with similar geological settings.

2. Regional geological setting

The Yangtze Platform is located in the northern part of south China and covers over 800,000 km², between the Qinling-Dabie orogenic belt to the north and the Cathaysian suture to the southeast (Fig. 1). The Yangtze Platform has a long history of continuous deformation and amalgamation due to the interaction of micro-blocks (the Cathaysian Block, Simao Block, Songpan Block, North China Block, and other orogenic belts) (Ma *et al.*, 2004; Hao *et al.*, 2013; Guo and Liu, 2013; Zhang, 2013a; Ju *et al.*, 2014). Many large

petroleum basins, for example, the Sichuan Basin (including the Chuanbei, Chuanxinan and Chuandongnan depressions) in the Upper Yangtze, the Jiangnan Basin in the Middle Yangtze, and the Subei Basin in the Lower Yangtze, are part of the Yangtze Platform (Fig. 1). The sedimentary basins and the orogenic belts are closely coupled: the Mesozoic Sichuan Basin is paired with the Longmenshan orogeny (220–130 Ma), Mesozoic Jiangnan Basin is coupled with the Qinling-Dabie Orogen (approximately 240–210 Ma), and Subei Basin and other rift basins in eastern China are coupled with the regional extension and Tan-Lu strike-slip movement in eastern China during the Meso-Cenozoic Era (Wang and Mo, 1995; Hsu and Chen, 1999; Wan, 2011).

The Yangtze Platform began filling with sediments 0.75–0.635 Ga in the Nanhua system (Ren *et al.*, 2013). It contains 6–12 km of Precambrian Ediacaran (Sinian, 635–540 Ma) to Cenozoic organic-rich and organic-lean sediments that are exploration targets for all hydrocarbon types (Fig. 2). The Yangtze Platform experienced a long history of continuous deformation and amalgamation, which has resulted in a very complex tectono-stratigraphic framework of passive margin basins superimposed with foreland and rifted basins (Wang and Mo, 1995; Kenneth and Chen, 1999; Wan, 2011) (Fig. 3). Regional subsidence has resulted in thick sandstone, carbonate, and shale deposition in the Yangtze Craton in the passive margin of Yangtze Platform from the Late Pre-Cambrian Ediacaran (Sinian) to the Ordovician Period

(Wang and Li, 2003). The Sinian Doushantuo formation and Early Cambrian Qiongzhusi formation (and its time-equivalent organic-rich shales) were widely deposited in shelf-to-abyssal settings in the Yangtze Platform during a period of sea level rise (Fig. 2). During the Ordovician-Carboniferous, the Yangtze Platform evolved into a foreland marine basin resulting from the Guangxi (Caledonian) orogeny (approximately Early-Middle Silurian in age), due to the Yangtze Craton collision with the Cathasian block. The organic-rich shale, marl, silty shale, and sandstone were regionally deposited in shoreline and shelf-to-slope settings. The western Upper Yangtze (western Sichuan Basin) was uplifted for short intervals during the Yunnan movement (Hercynian) (early Permian) and Dongwu movement (late Permian). Long-term uplift occurred after the Middle Triassic Period. The Qinling-Dabie orogenic belts experienced similar short uplift during the Late Paleozoic Era and long-term uplift after the Middle Triassic (240–210 Ma) (Figs.1 and 2). These Paleozoic to Early Triassic collisions and tectonic activities moderately deformed the sedimentary cover of the Yangtze Platform and produced only minor synorogenic magmatism (Vernhet, 2005; Li and Li, 2007). Generally, most Lower Paleozoic rocks were preserved with no obvious deformation (Figs. 3A and 3B). Later Indosinian (Triassic to Jurassic), Yanshanian (Jurassic to Cretaceous), Tan-Lu strike-slip, and Himalayan (Cenozoic) tectonic movements substantially influenced and disrupted the basins in the Yangtze Platform. Extensive thrusting, uplift, and erosion were accompanied by regional extension, especially strike-slip

tectonics, and volcanic intrusions and extrusions (Li and Li, 2007; He *et al.*, 2011; Jin *et al.*, 2013). Many Meso-Cenozoic lacustrine basins were also formed after the Late Triassic Period. For example, the foreland Sichuan Basin in the Upper Yangtze began to form in the Late Triassic, and rifted lacustrine basins were formed in the Middle and Lower Yangtze during the Cretaceous to Cenozoic Periods, (the Jiangnan Basin, Nanxiang Basin, and Subei Basin; Fig. 1s, 3A and 3B). The organic-rich lacustrine shales associated with coal, sandstone, and siltstone were deposited in swamp and shallow lake settings in the Mesozoic foreland basin and a semi-deep lake in the Cenozoic rifted basin (Figs. 2, 3A, and 3B).

In the Yangtze Platform, there are seven primary regional shale source rock intervals targeted for shale gas exploration: the Pre-Cambrian Sinian, Lower Cambrian, Upper Ordovician, Lower Silurian, Permian, Upper Triassic and Lower Jurassic (Fig. 2, Zou *et al.*, 2010). In this study, we focus on the Lower Cambrian and Lower Silurian marine shales, where industry exploration is focused. We chose the Qiongzhusi-equivalent shale to represent shales deposited during early Cambrian (ca. 529-514 Ma) (Zhang *et al.*, 2016), and the Longmaxi-equivalent shale to represent shales deposited during early Silurian (ca. 447.62-438.13 Ma) (Chen *et al.*, 2018). In the Yangtze Platform, the Upper Ordovician Wufeng-equivalent shale and Lower Silurian Longmaxi-equivalent shale are considered to be the same black-shale succession. Both are graptolite-bearing, organic-rich, and

carbonaceous-siliceous black shales, and only a subtle erosional surface or regional disconformity separates the two shale intervals. Hence, it is very difficult to subdivide the two-vertically consecutive shales. As the Ordovician shale is only distributed in the south-to-southwestern Sichuan Basin at 2–8 m thickness, and the Silurian Longmaxi shale has a thickness of 50–550 m (Jiang *et al.*, 2015, 2016), here we use the Silurian Longmaxi-equivalent shale to illustrate the regional distribution and shale gas potential of the Upper Ordovician to Lower Silurian shale interval.

3. Data and methodology

Data for this study were obtained from 37 measured outcrops, 600 core and outcrop samples, 128 wells (including 32 recently-drilled shale gas wells, and the production data, formation tests and reservoir data of 12 recently-drilled wells), as well as 18 previous industry reports and published literature. These data were regionally distributed across various tectonic and depositional settings throughout the Yangtze Platform (see Fig. 1, 6, 9, and 14 for locations of key wells and outcrops). Outcrops and cores from key wells were described for lithofacies and depositional environments. Collected shale outcrop and core samples from the Upper to Lower Yangtze areas were measured for geochemical parameters, gas content, mineralogy, and rock fabrics. The measured geochemical data for the lower Cambrian shale from typical wells and outcrops (including type section) of the Lower Cambrian

shale in Zhalagou, Sandu, Guizhou are listed in Table 1. The geochemical data for the lower Silurian shale from representative wells and outcrops are compiled in Table 2. The geochemical, gas content, and mineralogical measurements for typical Lower Silurian Longmaxi shale from core samples of the first successful Jiaoye1 well (located in the southeast of Sichuan Basin) are reported in Table 3.

Each shale property was measured in the same laboratory using the same instrument to ensure data consistency. Both the Lower Qiongzhusi-equivalent shale and the Lower Silurian Longmaxi-equivalent shale exhibit very high thermal maturities with equivalent vitrinite reflectance (R_o) ranging from 1.3%–5.7% (Ma *et al.*, 2004; Zou *et al.*, 2011; Hao *et al.*, 2013). The equivalent vitrine reflectance (R_o) values varies, as there were no vitrinite macerals for both Cambrian and Silurian shales and different researchers used different methods to calculate the equivalent vitrinite reflectance. Here, we use the equation of $R_o = 0.618(BR_o) + 0.4$ (where R_o = equivalent vitrinite reflectance values and BR_o =bitumen reflectance values) (Jacob, 1989) to calculate the equivalent R_o values for our core and outcrop sample measurements for the Lower Cambrian and Lower Silurian shales in the southeastern Sichuan Basin and the Yangtze Platform outside the Sichuan Basin. The calibrated results ranged from 1.35% to 4.31% for Cambrian shale and from 1.30% to 3.57% for Silurian shale (Tables 1-3).

We employed the “reservoir prediction” approach within a sequence

stratigraphic framework built from regional- to local-scales. First, the regional geologic history was synthesized to focus on the complex tectonic and depositional history of shale resources. Second, the regional tectono-stratigraphic cross-sections were generated to infer variations in tectonic complexity based on outcrop investigations, regional seismic reflection profiles, and subsurface correlation. Third, Paleozoic shale facies in different areas were identified based on outcrop measurements, core description, completion reports, well log interpretations, and petrographic analysis. Basin-scale variations on depositional facies, geochemistry, and thickness of the Lower Paleozoic shales were assessed across the Yangtze Platform by mapping shale geological and geochemical properties, stratigraphic correlation, and sequence stratigraphic analysis. Reservoir development was then predicted within a sequence stratigraphic framework, based on the correlation of shale properties exemplified by key outcrops and wells; Fourth, the Yangtze Platform was divided into different tectonic regions based on the burial history and tectonic stability. Relationships between shale reservoir properties and shale gas production in different depositional and tectonic settings were analyzed to reveal how depositional facies and structural activities influence shale reservoir properties and shale gas accumulation, preservation, and production.

4. Results of the depositional setting and distribution analysis of the Lower Paleozoic shales

Previous studies on the depositional environments of the Lower Paleozoic shales were limited to regional gross depositional environments (epoch time span, e.g., Lower Silurian) and only based on local outcrop investigations and limited drilling results (Lu, 1979; Su *et al.*, 2002; Feng *et al.*, 2004; Ma *et al.*, 2004; Liu *et al.*, 2013; Ju *et al.*, 2014). These analyses concluded that the Lower Cambrian Formation was deposited in a passive margin setting and the Lower Silurian Formation was deposited in a foreland setting (Ma *et al.*, 2004). Much disagreement exists regarding the gross depositional models previously constructed, and many terms (for example, “deepwater shelf;” Ma *et al.*, 2004; Guo, 2013) are not standard nomenclature. We identified and named individual facies for both Lower Cambrian Qiongzhusi-equivalent and Lower Silurian Longmaxi-equivalent shales from proximal to distal sediment source locations across the Yangtze Platform by integrating data from 37 outcrop investigations of shale reservoir intervals, including core descriptions, sample tests of recently drilled wells, lithologic analyses, and correlated well logs.

To better understand facies variations, we use a refined model (generated based on our integrated depositional study for shales in different tectonic settings) to help envision and describe the facies characteristics for the Lower Paleozoic shales across a range of depositional and tectonic settings in the Yangtze Platform (Fig. 4). The data illustrated in Fig. 4A describe the facies model for the Lower Cambrian Qiongzhusi-equivalent

shale from the shoreline environment in the northwestern Yangtze Platform to the abyssal environment in the southeastern Yangtze Platform. The data in Fig. 4B illustrate the facies model for the Lower Silurian Longmaxi-equivalent shale from the shoreline environment in the northwest to the foredeep environment in the southeast. We use commonly-accepted terminology (such as “intra-shelf low”) for both the Cambrian and Silurian shales to concisely describe the facies characteristics according to paleogeography and lithofacies features.

The Lower Cambrian Qiongzhusi shale and its age-equivalent interval facies include the following characteristics:

- 1) Shoreline facies: shaley siltstone and sandstone interbedded with shale
- 2) Shallow shelf facies: characterized by silty shale (Fig. 5A)
- 3) Intra-shelf low facies: organic-rich shale with phosphate nodules, sometimes interbedded with silty laminae (Fig. 5B)
- 4) Platform facies: marl or carbonate interbedded with shale
- 5) Slope facies: organic-rich siliceous shale
- 6) Slope-to-basinal facies: characterized by chert (Fig. 5C)
- 7) Abyssal facies: thin-bedded sandstone turbidities within shale (Fig. 5D)

The identified facies for the Lower Silurian Longmaxi shale and its age-equivalent interval included the following:

- 1) Intra-shelf facies: Widely distributed in Upper and Middle Yangtze Platform and the current exploration target. The lithology was characterized by organic-rich siliceous shale (Fig. 5E). The “intra-shelf

low area” is equivalent to the “backbulge depositional zone” proposed by DeCelles and Giles (1996) for foreland basins.

- 2) Shallow shelf facies: shale with siltstone interbeds (Fig. 5F)
- 3) Tidal flat and lagoon facies: marl, shale, dolomite and gypsum
- 4) Sandy foredeep facies: characterized by shoreline to deepwater sandstone (Fig. 5G), shaley siltstone and siltstone with shale
- 5) Organic-lean shale facies: in the distal foredeep, influenced by clastic dilution (Fig. 5H)
- 6) Organic-rich shale facies: in the distal foredeep that are far away from clastic dilution

4.1 Lower Cambrian Qiongzhusi-equivalent marine shale in the Yangtze Platform

The Lower Cambrian Qiongzhusi-equivalent shale was deposited in shallow shelf to abyssal settings. The shale, which ranges in thicknesses from 20–100 m, is distributed extensively in the Yangtze Platform. The interval isopach shows this shale generally thickens from the shallow northwest shelf toward an intra-shelf low and slope in the southeast (Fig. 6). The depocenter mainly includes the Sichuan Basin and surrounding areas between Chengdu and Guiyang in Upper Yangtze, in an area to the southwest of Wuhan in Middle Yangtze and close to Hangzhou in the Lower Yangtze. The average TOC range for the lower Cambrian Niutitang-equivalent shale in the Yangtze Platform was generally 2%–7%, although some intervals of the Niutitang

formation in Guizhou and Hunan Provinces may have higher TOC contents (up to 15%; Fig. 6). Based on the overlay map of depositional facies, TOC, and thickness, the intra-shelf low and slope accumulated thicker shale deposits with high TOC (> 2%) (Fig. 6).

Stratigraphic correlation for Lower Cambrian formations from the Upper to the Lower Yangtze Platforms shows the interfingering of lithofacies. The lithology and facies of lower Cambrian Qiongzhusi shale and equivalent strata (Jiulaodong, Niutitang, Muchang, Shuijingtuo and Hetang formations) vary in time and space. The black (organic-rich) shales in intra-shelf lows and slope settings are mainly distributed in the lower section of the Lower Cambrian Formations. The lithofacies evolved upward from dark shale to grey shale interbedded with siltstone, silty shale, marl, dolomite and limestone. This variation in facies reflects an evolution from intra-shelf low (in the lower part of the Cambrian interval) upward to a shallow shelf, shoreline and tidal flat (Fig. 7).

The detailed vertical changes in lithology, facies, mineralogy, and geochemistry is represented by a type section of Lower Cambrian shale in Zhalagou, Sandu, and Guizhou. The Lower Cambrian organic-rich shale has a sharp contact with its underlying argillaceous dolomite in the Pre-Cambrian Sinian Dengying Formation. The shales in the Lower Cambrian Zhalagou Formation and its overlying Middle Cambrian Douliujiang Formation evolve from siliceous organic-rich shale at the bottom, carbonaceous shale in the

middle, to gray shale at the top (Fig. 8). Field measurements using a SatisGeo GS-512 Gamma Ray Spectrometer, and TOC and X-ray-diffraction measurements in the laboratory indicated that the uranium (U), TOC and quartz content generally decreased upward in the Zhalagou (Qiongzhusi equivalent) shale interval. The lower Zhalagou shale demonstrated high U readings (nearly 80 ppm), TOC up to 10% in weight, and quartz content up to 45% (Fig. 8). This Lower Zhalagou (Cambrian Qiongzhusi-equivalent) shale is interpreted as a 3rd order depositional sequence based on changes in lithofacies, TOC and gamma ray values, and principles of the shale sequence (Jiang *et al.*, 2018). In the transgressive systems tract (TST), siliceous organic-rich shale (with TOC content of 2–10%) was deposited in slope to abyssal settings, and the TOC and uranium readings increased upward and reached maximum at maximum flooding surface (MFS). The early highstand systems tract (EHST) was also dominated by organic-rich black shale (though TOC was reduced compared to the TST). Uranium and TOC measurements decreased upward. The late highstand systems tract (LHST) was characterized by gray shale interbedded with silty shale and with TOC content further reduced (< 2%). The best shale gas reservoirs are typically found in the organic and brittle mineral-rich shales (e.g., Loucks and Ruppel, 2007). The vertical variations of shale properties indicated that the TST and EHST shales have the best reservoir quality for the Lower Cambrian Qiongzhusi-equivalent shale in the Yangtze Platform. Regionally, the overlay of shale facies,

thickness, and TOC shows the best Lower Cambrian shale gas potential was located in the southeastern, eastern, and northeastern Sichuan and northern Guizhou in the Upper Yangtze Platform, the western and southern Hubei and western Hunan in the Middle Yangtze Platform, and the western Zhejiang and southern Anhui in the Lower Yangtze Platform (Fig. 6).

4.2. Lower Silurian Longmaxi-equivalent marine shale in the Yangtze Platform

During the Silurian period, the Yangtze Platform was affected by strong quasi-symmetrical intracontinental shortening involving the sedimentary cover of the rift and its margins, as well as the basement (Hsu, 1990; Vernhet, 2013). The Lower Silurian Longmaxi-equivalent shale was mainly deposited in shallow shelf, intra-shelf lows and foredeep settings, with net thicknesses of 20–140 m, and is widely distributed in the Yangtze Platform. The isopach shows thickening generally from shoreline, shallow shelf and proximal foredeep toward an intra-shelf low and distal foredeep away from the foredeep and shoreline. The average TOC for the lower Silurian shale of the Lower and Middle Longmaxi Formations in the Yangtze Platform ranges from 1% to 2%. Based on the overlay map of the depositional system, TOC and thickness, the intra-shelf low and distal foredeep areas away from the clastic dilution were accumulated by shale with average to high TOC (> 2%) and thickness > 40 m (Fig. 9).

The stratigraphic correlation for the Lower Silurian Longmaxi-equivalent shale formation from the Upper Yangtze Platform to the Lower Yangtze Platform shows that the predominant system is an interfingering of lithofacies with delta progradation and clastic dilution in the foredeep setting in the Lower Yangtze Platform. The lithology and facies of the lower Silurian Longmaxi shale and its equivalent Gaojiabian shale vary in time and space. The black (organic-rich) shales in the intra-shelf low and distal foredeep areas (away from the proximal foredeep and shoreline settings with clastic influx) are mainly distributed in the lower section of the Lower Silurian equivalent formation. The lithofacies evolved from the dark shale upward to gray shale interbedded with calcareous shale in the Upper Yangtze Platform (e.g. Gongshen1 well, Zishen1 in Fig. 10), and siltstone and shaley siltstone in the Middle Yangtze and Lower Yangtze platforms (e.g., Jing101 well and Shengke1 well in Fig. 10). The deposition generally changed from an intra-shelf low in the lower part of the Lower Silurian Longmaxi shale interval upward to a shallow shelf in the Upper and Middle Yangtze areas, and changed from a distal foredeep environment to prograding sandy delta deposits and turbidites in a proximal foredeep sourced from the Cathasian Platform to the SE Yangtze Platform (Fig. 10).

The detailed vertical change in lithology, facies, mineralogy and geochemistry for the Silurian Longmaxi marine shale can be seen in a type well, the Jiaoye1 well in Sinopec's Jiaoshiba Gas Field in Fuling, Chongqing,

southeastern Sichuan Basin, and the Upper Yangtze Platform (Fig. 11). The Lower Silurian Longmaxi shale was deposited in a third-order depositional sequence. During the transgressive systems tract (TST), siliceous organic-rich shale, with TOC of 3%–5% and high gamma ray readings, were deposited in intra-shelf lows. The average quartz content was greater than 45% (>50% at the bottom). The early highstand systems tract (EHST) was also dominated by organic-rich black to grey shale with TOC 2%–4%, and the late highstand systems tract (LHST) was characterized by gray shale interbedded with silty shale and siltstone with low TOC content (< 2%) and low gamma-ray readings. As TOC and gamma ray values decreased, the quartz and gas contents correspondingly decreased upward in the Longmaxi shale interval (Fig. 11). Similar to the Lower Cambrian Qiongzhusi-equivalent shale, the TST and EHST intervals have the best reservoir quality. Regionally, the overlay of shale depositional system, thickness, and TOC shows the best Lower Silurian shale gas production zones are located in the southern, southeastern, and eastern Sichuan Basin in the Upper Yangtze Platform, northeastern Guizhou in the Upper Yangtze Platform, western and southern Hubei and western Hunan in the Middle Yangtze Platform, and Central Jiangsu to southeastern Anhui in the Lower Yangtze Platform (Fig. 9).

5. Results of the tectonism in the Yangtze Platform and control on lower Paleozoic shale gas generation, accumulation and preservation

As discussed at the beginning of this chapter, the Yangtze Platform has experienced multi-stage tectonic events, especially during the Early Paleozoic Guangxi (Caledonian) in the Silurian to the Cenozoic Himalayan tectonic movements. Tectonic influences have mostly exerted control through flexural effects of deformational loading.

As introduced in the regional geological setting, The tectonic history of the Lower Paleozoic marine shales in the Yangtze block has a generally more complex tectonic history than shales in USA even though the depositional history and characteristics of the organic-rich shale in the Lower Yangtze Platform are similar to organic-rich Devonian Marcellus shale and Mississippian Barnett shale deposited in distal foredeep and paleo-low areas coeval with orogenies that formed foreland basins (Ettensohn and Lierman, 2012; Jiang *et al.*, 2015, 2016).

The Qiongzhusi-equivalent Cambrian and the Longmaxi-equivalent Silurian shales have experienced at least four stages of deformation, including the Guangxi (Caledonian), Indosinian-Early Yanshanian (Triassic to Jurassic), Late Yanshanian-Early Himalaya (Cretaceous to early Paleogene), and Late Himalayan (Neogene to current) tectonic events (Jiang *et al.*, 2015, 2016). The Zhaotong shale gas demonstration zone in the Upper Yangtze Platform can be used as a typical example to reflect the tectonic stages. We identified structural traces of tectonic events from different geologic ages via surface geological surveys conducted in the Zhaotong shale gas demonstration zone

and surrounding areas. Guangxian (Caledonian) tectonic event resulted in the development of nearly EW- to NE-oriented folds, due to the collision between the Yangtze Block and the Cathaysia Block. Structural traces typified by this deformation can be observed in the middle Guizhou and Jiangnan-Xuefeng uplift in the Southern and Eastern margin of the Yangtze block (Fig. 12A).

During the Indosinian-Early Yanshanian tectonic event caused by the collision between the Yangtze block and Cathaysia Block to the southeast (and the North China block to the north), the northern margin of the Yangtze block and the southeastern margin experienced deformations resulting in the development of NW-EW- and NE-NEE-trending fold traces (Fig. 12B). During the Late Yanshanian-Early Himalayan tectonic event, the Yangtze block collided with the North China and the Qinghai Tibet block, which resulted in the development of NW and NNW trending structural traces (Figs. 12C and 4D).

During the Late Himalayan tectonic event, the collision between the Indian plate, Qinghai Tibet block, North China block, and Yangtze Formation generated NS-trending thrusts and strike-slip structural traces (Fig. 12D).

These Yanshanian and Himalayan structural traces, superimposed with the Guangxian (Caledonian) and Indosinian structural traces, occur in the western margin of the Yangtze block, near the Sanjiang orogenic belt and southwestern Sichuan depression (Fig. 12D). This area also bears evidence of cross-cutting structures from different stages. The southeast portion of the Zhaotong demonstration zone (in the south Sichuan Basin) is mainly composed of

NNE-trending folds and faults (Fig. 13). The northwest portion is dominated by EW- and NNW-trending folds and faults, which reflects the development of EW-NE-trending folds during Guangxian (Caledonian) and Indosinian-Early Yanshanian stages. The development of NNW structures indicate they were formed during Late Yanshanian-Early Himalayan stage. The NS-trending strike slip faults and associated folds were formed during the Late Himalayan stage (Fig. 13). These multi-stage and multi-orientated tectonic activities facilitated the development of extensive natural fractures with multiple orientations, which may accommodate the accumulation of shale gas or result in leaking.

However, these multi-stage tectonic events did not reshape the Yangtze Platform evenly in all areas. Based on the times of tectonic movements and intensities, we divided the Yangtze Platform into the following three different tectonic regions (Fig. 14):

- (I) relatively stable tectonic areas, which experienced two tectonic movements with regional uplift;
- (II) transitional tectonic areas (between stable and active), which experienced three tectonic movements;
- (III) active tectonic areas, which experienced at least four tectonic movements.

Reconstruction of the burial histories of three representative wells (the Dingshan1 in the Upper Yangtze, Paishen1 in the Middle Yangtze, and Yan 1 in the Lower Yangtze Platform) with calibrations of newly measured maturity

are included to illustrate the characteristics of each region with different tectonic intensities (Fig. 14). Multi-stage subsidence and uplift resulted in different thermal and hydrocarbon-generation histories.

The Dingshan1 well in the Upper Yangtze Platform, located in a relatively stable tectonic area in the Yangtze Platform, exhibited two major uplift and erosion events during the Late Silurian and Late Cretaceous Periods (Fig. 14A). The onset of oil generation (green color in Fig. 14) in the Cambrian shale began in the Early Ordovician Period; gas (red color in Fig. 14) began to generate in the Early Jurassic Period and reached a peak in the Cretaceous Period, due to the high maturity of the source rock. Initiation of oil generation from Ordovician to Silurian shale started in the Early Jurassic Period, due to a long period of uplift and erosion from the Late Silurian to Early Permian periods. Gas then started to generate in the Early Cretaceous. The earliest-generated oil was later thermogenically cracked to dry gas in the Cretaceous Period. Oil generated and accumulated from Cambrian shales may have been partially breached by Late Silurian uplift, and potential gas reservoirs could have been partially disrupted by the later major uplift since the Late Cretaceous Period, which eroded rocks of approximately 3000 m thickness. Gas generation and accumulation from the Ordovician to Silurian shale sections were influenced by only one tectonic disruption since the Late Cretaceous Period.

The Paishen1 well in the Middle Yangtze Platform is located in a transitional tectonic area with three periods of uplift and erosion occurring in

the Late Silurian, Late Jurassic and Late Paleogene Periods (Fig. 14B). The onset of oil generation from the Cambrian shale started in the Late Silurian Period, then gas began to generate in the Late Permian, reaching a peak in the Triassic. Initiation of oil generation from the Ordovician to Silurian shales started in the Early Permian, and gas began to generate in the Late Triassic Period. All the early-generated oil was thermogenically cracked to dry gas in the Jurassic Period. The accumulated gas from both the Cambrian and Ordovician-Silurian shales may have been breached twice; once by the Late Jurassic uplift and again during the Late Paleogene uplift.

The Yan 1 well in the Lower Yangtze Platform is located in an active tectonic area which has experienced at least four episodes of uplift and erosion during the Late Silurian to Middle Devonian periods (Guangxi or Caledonian movement), Late Triassic to Early Cretaceous periods (Indosinian and Yanshannian movements), and Paleogene to Neogene periods (Himalayan movements) (Fig. 14C). The onset of oil generation from Cambrian shales began in the Early Silurian Period, with gas generation initiating in the Late Permian Period and reaching a peak in Late Triassic Period. Oil generation from the Ordovician-Silurian shales began in the Late Silurian Period and gas began to accumulate in the Triassic Period, following the second period of oil generation due to burial after the Caledonian uplift from the Late Silurian to Middle Devonian periods. All the early-generated oil was thermogenically cracked to dry gas in the Early Cretaceous Period. Generally,

both the Cambrian and Ordovician-Silurian shales experienced multi-stage subsidence and uplift, and the oil and gas accumulated at earlier times may have breached at least four times between the Late Silurian to the Neogene periods.

Tectonic movements thus played critical roles for both conventional and unconventional hydrocarbon preservation. The extensive organic-rich Lower Cambrian and Lower Silurian marine shales only contributed minorly to conventional oil and gas production in the Yangtze Platform in southern China (Ma *et al.*, 2004). Recognizing that the marine organic-rich shales in China are located in more active tectonic settings than U.S.-producing marine shales, it was concluded that shale gas may have been lost in open systems due to several episodes of intense post-generation tectonic movements (Hao *et al.* 2013). The stable tectonic area in the Upper Yangtze Platform appears to be more favorable for shale gas preservation than the transitional tectonic area in the southern portion of the Upper Yangtze Platform, Middle Yangtze Platform, or the tectonically active area of the Lower Yangtze Platform. The Lower Yangtze area may have the least amounts of shale gas preserved in the Lower Paleozoic marine shale sections, due to its location within the most active tectonic setting, where at least four major tectonic disruptions are known.

Gas content data and total organic carbon (TOC) demonstrate that the gas content in the Lower Paleozoic marine shales in the Yangtze Platform are generally lower than in most U.S. marine producing shales and is relatively

close to the gas content in the Marcellus shale (Fig. 15). This supports a stable tectonic setting for most U.S. marine shales (Hao *et al.* 2013). The Appalachian Basin, where the Marcellus Shale is located, has experienced four major continuous tectonic disruptions and is more tectonically active than most U.S. basins (Ettensohn and Lierman, 2012), which explains why the shale gas content in the Marcellus is lower than that in other US shales, given the same TOC contents. Further analysis of these data indicate that the gas content has a positive correlation with TOC for all major marine shales in China and the U.S., and suggests that TOC has a crucial role in gas generation and gas content (accumulation) as free gas in organic pores or adsorbed gas onto organic matter (Ross and Bustin, 2007; Loucks *et al.*, 2009; Milliken *et al.*, 2013).

We also found that the shale gas content in the Longmaxi shale from the Jiaoye1 well was consistently higher than that from Pengye1 well, given the same TOC value and same intra-shelf depositional setting (Fig. 15). This observation prompted us to investigate what caused the difference for the shales with the same geochemical and depositional properties. Two schematic cross-sections from the stable tectonic areas inside the Sichuan Basin to the transitional tectonic areas (with tight synclines and many faults) show the distinct variations in formation pressure and initial shale gas production rates across different regions (Fig. 16). The data in Fig. 16A illustrate a profile across the Jiaoye1 well in the Jiaoshiba Shale Gas Field in Fuling to the Pengye1 well

in the Sanzheping syncline in Pengshui, Chongqing. Both production rate and formation pressure drop dramatically from the stable tectonic area (Jiaoshiba Shale Gas Field) to the transitional tectonic area that is represented by tight synclines and many faults. The highest reported shale gas production rate in China, with 547,000 m³/day (19 MMcf /day), occurs from the Silurian Longmaxi marine shale, with a pressure coefficient of 1.55, in the Jiaoye8-2HF horizontal well in the Jiaoshiba Shale Gas Field. The vertical shale gas wells (e.g., the Jiaoye1 well) in this area have high production rates of 200,000 m³/day. The Pengye HF-1 horizontal well to the southeast has a production rate of only 25,000 m³/day from the same Longmaxi shale with a pressure coefficient of 0.95.

The data in Fig. 16B illustrate a profile across the Ning201 well in the Changning pilot shale gas area inside the Sichuan Basin (stable tectonic area) to the Zhao101 well in Zhaotong pilot shale gas area. Reverse faults and tight synclines with a similar decreasing trend in pressure and production rates as seen in the Jiaoshiba Shale Gas Field to the Pengshui area supports the effects of tectonic history. The Ning201-H1 horizontal well, located in a stable tectonic area, has a high production rate of 180,000 m³/day from the Silurian Longmaxi shale, with a pressure coefficient of 2. The Zhaotong104 well southwest of the Ning201-H1 is located in the periphery of the Sichuan Basin, close to a tectonically-complex area marked by many reverse faults and tight synclines. Production from the Longmaxi shale in the Zhaotong104 well drops

to 10,000 m³/ day with a pressure coefficient of 1. The Zhao103 well, located in the limb of a tight syncline and close to a reverse fault, has no production from the Longmaxi shale. These results, from the tectonically-stable to the tectonically-complex areas, reveal that both shale gas production and shale-formation pressure are likely related to tectonic activities. Tectonic movements apparently breached the Paleozoic marine shales in the Yangtze Platform, allowing leakage of part of the accumulated shale gas. This most likely contributed to the reduction in formation pressure. The transitional tectonic area outside the Sichuan Basin has had at least three intense tectonic movements creating tight synclines and many faults (Fig. 14); these events caused the loss of free gas and a decrease in formation pressure. Based on the free shale gas modeling for the Paleozoic shales in the southern Sichuan Basin in the Upper Yangtze Platform (Zhou *et al.*, 2014), the maximum free gas content in the Lower Silurian shale is 4.23 m³/ton during its maximum burial, and the present shale gas content in this shale is 2.77 m³/ton with a total drop of approximately 34.5% due to 4,300-m uplifting in the relatively tectonically-stable area. The shales in the Middle Yangtze and the Lower Yangtze platforms are susceptible to more active tectonic movements, and more free shale gas was lost due to multi-stage strong uplifting. Hence, current gas accumulation in complex tectonic areas (e.g., the Marcellus shale in the Appalachian Basin and shales in this study) is lower (Fig. 15), resulting in lower production rates from shale reservoirs with partial gas and pressure

loss. The tectonically-stable areas demonstrate high shale gas content and high rates of production due to the preservation of gas and high pressure (Fig. 16).

The structural characteristics illustrated by the data in Figs. 16A and 16B clearly indicate that the tectonically-stable area inside the basin was characterized by a broad, gentle syncline with local tight or broad anticlines, and a good shale gas preservation due to having the least amount of tectonic activity, faults and undisrupted Upper Paleozoic to Mesozoic cap rocks. Therefore, the tectonically-stable area experienced good shale gas accumulation, indicated by higher gas content, overpressure and the highest production rate. Areas close to the mountains associated with the Jiannan-Xuefeng orogenic event are characterized by intensive deformations, active faults cutting upward to the surface, extensive outcropping of Cambrian and Silurian shales, and very tight anticlines and synclines (Figs. 3, 16A, and 16B), which resulted in the shale gas leaking and no production. Some synclines outside the Sichuan Basin are only moderately disrupted by faulting and contain low-angle shale strata in the syncline center away from faults; these deposits have fair to good conditions for shale gas accumulation and production. Partial shale gas leaking caused by tectonic disruptions may have resulted in underpressurization of the reservoir and a correspondingly lower production rate compared to areas inside the basin (Fig. 16A).

6 Discussions

The distribution of high quality Lower Cambrian and Lower Silurian marine shales in the Yangtze Platform is controlled by the depositional environments. The marine shale, with high TOC and high brittle minerals, developed during the TST to EHST interval in the intra-shelf low to slope setting, far away from clastic dilution. The reduced gas content and production variation were mainly caused by tectonic settings. Intensive tectonic or structural activities generally disrupted shale gas accumulation, released overpressure, and resulted in lower production. Regional tectonically-stable areas inside the Sichuan Basin widely developed overpressure favorable for shale gas accumulation and production. Local areas away from mountain, fault, outcrop, and tight structures outside the Sichuan Basin are also favorable for overpressure development and production.

The tectonic control on shale gas accumulation can be further explained by comparing key parameters of shale gas-producing or emerging-production areas located in neighboring or similar depositional setting regions in the Upper Yangtze Platform (Table 4). The data in Table 4 indicate that the Zhaotong- Huangjinba, Channing, Weiyuan and Jiaoshiba/Fuling areas have similar properties of intra-shelf low facies, thickness, TOC range, porosity, clay content, and brittle index. However, the Zhaotong-Huangjinba area outside the basin has a slightly lower gas content, normal- to over-pressure in the syncline axis, a complex stress field and tectonic setting (shear compression and deformed complex structures), larger horizontal stress contrast (>20 MPa),

and many more fractures compared to the neighboring Changning, Weiyuan, and Jiaoshiba areas inside the basin. These indicate that the overpressure is widely developed inside the Sichuan Basin, and that overpressure can also develop in local areas outside the Sichuan Basin. The seismic reflection from the Changning shale gas demonstration zone (inside the Sichuan Basin) to the Zhaotong shale gas demonstration zone outside the Sichuan Basin clearly shows that the Zhaotong Block has more complex structure with tighter folds and more large-throw faults than the Changning Block (Fig. 17). Production data in the Zhaotong Block suggested that the area with pressure coefficients less than 1.2 is usually close to faults, and that the tight structure or outcrop has much lower production or no production. In contrast, the overpressure area with pressure coefficients greater than 1.6 in the syncline center has a daily production of over 20,000 m³. The YS111 well in the faulted tight structure with high-angle dipping shale has much lower pressure and almost no production, while the YS108 well area is located in the axis of a syncline bounded by two thrust faults in the northeast Huangjinba in the Zhaotong shale gas demonstration zone and the Lower Silurian shale lies at low-angle dip (Fig. 17), this well was tested to have the highest pressure (with a pressure coefficient of nearly 1.8) in the Zhaotong Block. The production rate of this well is about 200,000 m³/day, from a 26-stage horizontal lateral of 1,600-1,800m. The accumulated production in 2017 in the Zhaotong demonstration zone reached 0.5 billion cubic meters from the wells located in the local

overpressure areas in the Zhaotong Block. This suggests that the local areas with overpressure may be suitable for shale gas exploration and production in tectonically-complex areas.

7. Conclusions

This study reveals that the Lower Cambrian Qiongzhusi-equivalent organic-rich (TOC > 2%) shale was mainly developed in a transgressive systems tract (TST) and early highstand systems tract (EHST) deposited in the intra-shelf low to slope settings. The organic-rich (TOC > 2%) Lower Silurian Longmaxi-equivalent shale was also situated in the TST- and EHST- intervals deposited intra-shelf low area away from clastic dilution in a foreland basin setting.

The Yangtze Platform is located in a more complex tectonic setting than U.S. marine shales. The Yangtze platform was divided into three tectonic regions based on stages and intensities of tectonic activities: relatively stable tectonic areas (two major events), transitional tectonic areas (three major events), and active tectonic areas (four tectonic movements). The Sichuan Basin on the Upper Yangtze Platform is located in a relatively stable tectonic area with a broad syncline and gentle fold, and the high production of shale gas is from the regionally-overpressured shale in this area. The Upper Yangtze Platform outside the Sichuan Basin and the Middle Yangtze areas are located in a transitional tectonic setting, and shale gas produces at lower rates in the

slightly under-pressured synclines. Good- to fair-production in the tectonically-complex area only occurs from the overpressured area locally developed in the stable syncline center. Little or no production in areas close to faults, tight structure, outcrop, or mountains was observed.

The Lower Cambrian and Lower Silurian shales in the Yangtze Platform in China are similar to the Marcellus shale in the Appalachian Basin in the U.S.; both having lower gas content compared to areas with less tectonic complexity, such as the Haynesville, Barnett, and Woodford shales. These observations may imply that low gas content is an indication of their shared history of complex tectonic events. Favorable facies and overpressure in tectonically-stable areas of the Yangtze Platform likely indicates where the “sweet spot” for exploration and development is located.

ACKNOWLEDGEMENTS

We thank PetroChina for giving us the privilege to work on the industry data. The Natural Science Foundation of China (41728004), China National Giant Oil and Gas Program (2015ZX05068), CNPC Special Project (2012F-47-02), and EGI's (Energy & Geoscience Institute at the University of Utah) multi-year industry-sponsored China Shale Plays consortium funded this study. The international collaboration between PetroChina and EGI made this research and paper possible. Comments and help from Elinda McKenna, Anne Barrow, and Justin Whitney of the University of Utah and Jeff May (retired Chief Geologist of EOG Resources) during the preparation of this paper are appreciated.

References

Chen, X., Chen, Q., Zhen, Y., Wang, H., Zhang, L., Zhang, J., Wang, W. and Xiao, Z., 2018. Circumjacent distribution pattern of the Lungmachieian graptolitic black shale (early Silurian) on the Yichang Uplift and its peripheral region. *Science China-Earth Sciences.*, 61(9), 1195-1203

Curtis, J. B., 2002. Fractured shale-gas systems. *AAPG Bulletin*, 86(11), 1921–1938.

DeCelles, P.G. and K.A. Giles, 1996. Foreland basin systems. *Basin Research*, 8, 105-123

Du, X-B, Zhang, M-Q, Lu, Y-C, Ping, C, and Lu, Y-B, 2015. Lithofacies and depositional characteristics of gas shales in the western area of the Lower Yangtze, China. *Geological Journal*, 50, 683–701.

EIA (Energy Information Administration), 2011. World shale gas resources: An initial assessment of 14 regions outside the United States,

<http://www.eia.gov/analysis/studies/worldshalegas/pdf/fullreport.pdf> (accessed April 20, 2013).

EIA (Energy Information Administration), 2013. Technically Recoverable Shale Oil and Shale Gas Resources: An Assessment of 137 Shale Formations in 41 Countries Outside the United States,

<http://www.eia.gov/analysis/studies/worldshalegas/pdf/fullreport.pdf> (accessed

August 23, 2013).

Ettensohn, Frank R., Lierman, R.T., 2012. Large-scale tectonic controls on the origin of paleozoic dark-shale source-rock basins: Examples from the Appalachian Foreland Basin, Eastern United States, in D. Gao, ed., Tectonics and sedimentation: Implications for petroleum systems. AAPG Memoir 100, 95-124.

Feng, Z., Peng, Y., Jin, Z., 2004. Cambrian and Ordovician lithofacies paleogeography in China (in Chinese). Beijing: Petroleum Industry Press, 4-50

Guo,T., Liu, R., 2013. Implications from marine shale gas exploration break-through in complicated structural area at high thermal stage: Taking Longmaxi Formation in Well JY1 as an example(in Chinese with English abstract). Natural Gas Geoscience, 24(4), 643-651.

Guo, T., 2013. Evaluating of highly thermally mature shale-gas reservoirs in complex structural parts of the Sichuan Basin. Journal of Earth Science, 24(6), 863-873.

Hao, F., Zou, H., Lu, Y., 2013. Mechanisms of shale gas storage: Implications for shale gas exploration in China. AAPG Bulletin, 97(8), 1325-1346.

Hsu, K.J., Li, J., Chen, H.H., Wang, Q., Sun, S., Sengör, A.M.C., 1990.

Tectonics of South China: key to understanding west Pacific geology.

Tectonophysics, 183, 9–39.

He, Z., Wang, X., Li, S., Wo, Y., Zhou, Y., 2011. Yanshan Movement and its influence on petroleum preservation in middle-upper Yangtze region.

Petroleum Geology & Experiment, 33(1), 1-11 (in Chinese with English abstract).

Hill, D.G., Nelson, C.R., 2000. Gas Productive Fractured Shales: An Overview and Update. Exploration & Production: Gas TIPS, 7(2), 11-16.

Jacob, H., 1989. Classification, structure, genesis and practical importance of natural solid oil bitumen (“migrabitumen”). International Journal of Coal Geology, 11, 65-79.

Jarvie, D. M., 2012. Shale resource systems for oil and gas: Part 1—Shale-gas resource systems, in J. A. Breyer, ed., Shale reservoirs—Giant resources for the 21st century. AAPG Memoir 97, 69–87.

Jiang, S., 2014, Prospects for Shale Gas Development in China, in R. E.

Hester and R. M. Harrison, ed., Fracking. Royal Society of Chemistry,

Cambridge. ISBN: 978-1-84973-920-7, p.85-90.

Jiang, S., Zhang, J., Jiang, Z., Xu, Z., Cai, D., Chen, L., Wu, Y., Zhou, D., Jiang, Z., Zhao, X., Bao, S., 2015. Geology, resource potentials, and properties of emerging and potential China shale gas and shale oil plays, Interpretation, 3 (2) SJ1-SJ13

Jiang, S., Xu, Z., Feng, Y., Zhang, J., Cai, D., Chen, L., Wu, Y., Zhou, D., Bao, S., Long, S., 2016. Geologic characteristics of hydrocarbon-bearing marine, transitional and lacustrine shales in China. Journal of Asian Earth Sciences, 115, 404-418

Jiang, S., Zou, C., Dong, D., Lin, W., Chen, Z., Chen, L., Wu, L., Dang, W. and Li, Y., 2017. Sequence Stratigraphy of Fine-Grained "Shale" Deposits: Case Studies of Representative Shales in the USA and China, Seismic and Sequence Stratigraphy and Integrated Stratigraphy - New Insights and Contributions, Dr. Gemma Aiello (Ed.), InTech, 19-34, DOI: 10.5772/intechopen.71137.

Jin, Z., Yuan, Y., Liu, Q., Wo, Y., 2013. Controls of Late Jurassic-Early Cretaceous tectonic event on source rocks and seals in marine sequences, South China. Science China Earth Sciences, 56(2), 228-239.

Ju, Y., Wang, G., Bu, H., Li, Q., Yan, Z., 2014. China organic-rich shale geologic features and special shale gas production issues. *Journal of Rock Mechanics and Geotechnical Engineering*, 2, 1-12.

Li, Z., Li, X., 2007. Formation of the 1300-km-wide intracontinental orogen and postorogenic magmatic province in Mesozoic South China: a flat-slab subduction model. *Geology*, 5(2), 179–182.

Liu, S., Wang, S., Sun, W., Ran, B., Yang, D., Luo, C., Ye, Y., Bai, Z., Qiu, J., 2013. Characteristics of black shale in Wufeng Formation and Longmaxi Formation in Sichuan Basin and its peripheral areas. *Journal of Chengdu University of Technology(Science & Technology Edition)*, 40(6), 621-639 (in Chinese with English abstract).

Lu, J., 1979. The Cambrian sedimentary minerals in China and its environmental biology control (in Chinese): Beijing, Geological Publishing House, 75p.

Luning, S., Craig, J., Loydell, D.K., Storch, P., Fitches, B., 2010. Lower Silurian 'hot shales' in North Africa and Arabia: regional distribution and depositional model. *Earth-Science Reviews*, 49, 121-200.

Loucks, R.G., Ruppel, S.C., 2007. Mississippian Barnett shale: Lithofacies and depositional setting of a deep-water shale-gas succession in the Fort Worth Basin, Texas. *AAPG Bulletin*, 91(4), 579-601

Loucks, R.G., Reed, R. M., Ruppel, S.C., Jarvie, D.M., 2009. Morphology, genesis, and distribution of nanometerscale pores in mudstones of the Mississippian Barnett Shale. *Journal of Sedimentary Research*, 79, 848–861.

Ma, L., Chen, H. J., Gan, K. W., 2004. Tectonics and marine petroleum geology in south China (in Chinese). Beijing, China Geology Press, p. 37–41.

Mavor, M., 2003. Barnett Shale gas-in-place volume including sorbed and free gas volume, AAPG Search and Discovery Article #90010, AAPG Southwest Section Meeting, 1-4 March 2003, Fort Worth, Texas, USA. Tulsa.

Milliken, K.L., Rudnicki, M., Awwiller, D.N., Zhang, T., 2013. Organic matter-hosted pore system, Marcellus Formation (Devonian), Pennsylvania. *AAPG Bulletin*, 97(2), 177–200.

Ren, J.S., Niu, B.G., Wang, J., Jin, X.C., Zhao, L., Liu, R.Y., 2013. Advances in research of Asian geology - A summary of 1:5M International Geological Map of Asia project. *Journal of Asian Earth Sciences*, 72, 3-11.

Ross D.J.K., Bustin, R.M., 2007. Shale gas potential of the Lower Jurassic Gordondale Member, northeastern British Columbia. *Canada Bulletin of Canadian Petroleum Geology*, 55, 51–75.

Steward, D. B., 2007. The Barnett Shale play: Phoenix of the Fort Worth Basin—A history. The FortWorth Geological Society and The North Texas Geological Society, ISBN 978-0-9792841-0-6, 202 p.

Su, W., He, L., Wang, Y., Gong, S., Zhou, H., 2002. K-Bentonite beds and high-resolution integrated stratigraphy of the uppermost Ordovician Wufeng and the lowest Silurian Lonmaxi formations in South China. *Science in China (D)*, 2002, 32(3), 207-219

Tan, J., Horsfield, B., Fink, R., Krooss, B., Schulz, H., Rybacki, E., Zhang, J., Boreham, C.J., Van Graas, G., Tocher, B. A., 2014. Shale Gas Potential of the Major Marine Shale Formations in the Upper Yangtze Platform, South China, Part III: Mineralogical, Lithofacial, Petrophysical, and Rock Mechanical Properties. *Energy Fuels*, 28(4), 2322–2342

Vernhet, E., 2005. Sedimentary processes, evolution, and paleoenvironmental reconstruction of the southern margin of the Ediacaran Yangtze platform (Doushantuo Formation, central China). PhD thesis, Freie Universität Berlin, 172p.

Vernhet, E., 2013. The Neoproterozoic–Early Paleozoic tectonic evolution of the South China Block: An overview. *Journal of Asian Earth Sciences*, 74, 198-209.

Wan, T., 2011. *The Tectonics of China: Data, Maps and Evolution*: Beijing, Heidelberg, Dordrecht, London, New York, Higher Education Press and Springer, 501p.

Wang, F., He, Z., Meng, X., Bao, L., Zhang, H., 2011. Occurrence of shale gas and prediction of original gas in place (OGIP). *Natural Gas Geoscience*, 22(3), 501-510.

Wang, H.Z., Mo, X., 1995. An outline of the tectonic evolution of China. *Episodes*, 18, 6-16.

Hsu, K.J. and Chen, H.H., 1999. *Geologic atlas of China*: Amsterdam, Elsevier, 320 p.

Wang, J., Li, Z., 2003. History of Neoproterozoic rift basins in South China: implications for Rodinia break-up. *Precambrian Research*, 122, 141-158.

Zhang, J., Xu, B., Nie, H., Wang, Z., Lin, T., 2008. Exploration potential of shale gas resource in China. *Natural Gas Industry*, 28(6), 136-140 (in Chinese).

Zhang, D, Li, Y., Zhang, J., Qiao, D., Jiang, W., Zhang, J., 2012. National survey and assessment of shale gas resource potential in China(in Chinese). Beijing, Geologic Publishing House.

Zhang, H., Xu, X., Liu, W., Men, Y., 2013. Late Ordovician-early Silurian sedimentary facies and palaeogeographic evolution and its bearings on the black shales in the middle-upper Yangtze area: *Sedimentary Geology and Tethyan Geology*, 33(2), 17-24.

Zhang, Y. Y., He, Z. L., Jiang, S., Gao, B., Liu, Z. B., Han, B., and Wang, H., 2017, Marine redox stratification during the early Cambrian (ca. 529-509 Ma) and its control on the development of organic-rich shales in Yangtze Platform: *Geochemistry Geophysics Geosystems*, 18(6), 2354-2369.

Zhou, Q., Xiao, X., Tian, H., Pan, L., 2014. Modeling free gas content of the Lower Paleozoic shales in the Weiyuan area in the Sichuan Basin, China. *Marine and Petroleum Geology*, 56, 87-96.

Zou, C., Dong, D., Wang, S., Li, J., Li, X., Wang, Y., Li, D., Cheng, K., 2010.

Geological characteristics and resource potential of shale gas in China.

PETROL. EXPLOR. DEVELOP, 37(6), 641–653.

Zou, C., Dong, D., Yang, H., Wang, Y., Huang, J., Wang, S., Fu, C., 2011.

Conditions of shale gas accumulation and exploration practices in China (in

Chinese with English abstract). Natural Gas Industry, 31(12), 26–39.

ACCEPTED MANUSCRIPT

Table Captions

Table 1 Geochemical measurements for key wells and outcrops of Lower Cambrian Qiongzhusi equivalent shale in the Yangtze Platform. See Fig. 8 for locations of wells and outcrops.

Table 2 Geochemical measurements for key wells and outcrops of Lower Silurian shale (Lower to Middle Section of Longmaxi Formation) in the Yangtze Platform. See Fig. 11 for locations of wells and outcrops.

Table 3 Geochemical, gas content, and mineralogical measurements from core samples of JY1 well.

Table 4 Comparison of key parameters for shale reservoir quality and shale gas accumulation in different areas in Upper Yangtze Platform. See Figs. 16 and 17 for the locations of Jiaoshiba, Changning, and Zhaotong areas/blocks and Fig.1 for location of Weiyuan area/block.

Figure Captions

Fig. 1. Tectonic setting of Yangtze Platform in South China (compiled from Wang and Mo, 1995; Kenneth and Chen, 1999; Wan, 2011), showing the major orogenic belts and depositional depressions during the Paleozoic Period. Ages of orogenic activity are noted. Locations of key shale gas wells recently drilled and cross-sections for Figs. 3A, 3B, 14A, and 14B are also shown.

Fig. 2. Stratigraphic column and major tectonic episodes for Yangtze Platform (parital TOC of Cambrian and Silurian shales and sea level curve modified after Zou *et al.*, 2010).

Fig. 3. Regional tectono-stratigraphic frame work for Upper Yangtze Platform (A) and Lower Yangtze Platform (B). See Fig. 1 for locations of the two transects. Tecto-stratigraphic framework was compiled based on regional seismic reflections, outcrop investigations, and subsurface drilling data.

Fig. 4 Depositional models for the Lower Cambrian shale deposited in the passive margin setting (A) and the Lower Silurian shale deposited in the foreland setting (B). The models are proposed based on our basin analysis and facies identified using data from outcrop and wells gathered in this study. Regional tectonic and depositional setting is modified from Ma *et al.* (2004).

Fig. 5. Outcrop and core photos showing Lower Cambrian Qiongzhusi equivalent and Lower Silurian Longmaxi equivalent shales facies. Outcrop and core photos showing Lower Cambrian Qiongzhusi equivalent and Lower Silurian Longmaxi equivalent shales facies. A, Silty shale in a shallow shelf setting. Lower Cambrian Qiongzhusi equivalent, Niutitang shale outcrop in Jishayankong, Guizhou, Upper Yangtze; B, Organic-rich shale with phosphate nodules in an intra-shelf low setting. Lower Cambrian Qiongzhusi equivalent, Niutitang shale outcrop in Duodingguan, Weng'an, Guizhou, Upper Yangtze; C, Chert in an abyssal setting. Lower Cambrian Qiongzhusi equivalent-Niutitang shale outcrop in Zhalagou, Sandu, Guizhou, Upper Yangtze; D, Thin-bedded sandstone turbidite in an abyssal setting, Lower Cambrian Qiongzhusi equivalent, Niutitang shale outcrop in Longshan, Binyang, Guangxi; E, Organic-rich (TOC = 3.5%) siliceous shale in an intra-shelf low setting. Lower Silurian Longmaxi shale core at 2402 m from Jiaoye1 well in Fuling, SE Sichuan Basin; F, Shale with siltstone interbeds (TOC = 1.65%) in a shallow shelf setting. Lower Silurian Longmaxi core at 2338 m from the Jiaoye1 well in Fuling, SE Sichuan Basin; G, Deepwater turbidite sandstone in a foredeep setting, Lower Silurian Longmaxi equivalent – Gaojiabian Fm outcrop in Bailongtan, Hangzhou, Lower Yangtze; H, Organic-lean shale, Lower Silurian Longmaxi equivalent, Gaojiabian shale core at 3109.7 m from N8 well in Taizhou, Jiangsu, Lower Yangtze. Core photos E and F are courtesy of Y. Ma, Sinopec, 2013. See Figs. 1, 6 and 9 for well and outcrop locations.

Fig. 6. Spatial distribution of the depositional systems, thickness and total organic carbon (TOC) of Lower Cambrian Qiongzhusi equivalent shale in the Yangtze Platform and adjacent areas (thickness and TOC modified from Ma *et al.*, 2004 using new data from wells and outcrops. Some key wells and outcrops are shown on the map). The thick red line represents orogenic belt.

Fig. 7. Cross section demonstrating stratigraphic correlation and facies variations from the Upper Yangtze Platform to the Lower Yangtze Platform, showing the interfingering of lithofacies for the Lower Cambrian formations. The Lower Cambrian Qiongzhusi equivalent strata include Jiulaodong, Niutitang, Muchang, Shuijingtuo and Hetang formations. See inset map for location of the cross section.

Fig. 8. Measured type outcrop of the Lower Cambrian Qiongzhusi equivalent, Zhalagou shale in Zhalagou, Sandu, Guizhou. FS=flooding surface, TST=transgressive systems tract, HST=highstand systems tract, EHST=early highstand systems tract, LHST=late highstand systems tract, MFS=maximum flooding surface. See Fig. 5 for the location of the outcrop.

Fig. 9. Depositional system, thickness and TOC of Lower Silurian Longmaxi equivalent shale in the Yangtze Platform and adjacent area (thickness and TOC modified from Ma *et al.*, 2004 using new data from wells and outcrops.

some key wells and outcrops are shown on the map).

Fig. 10. Stratigraphic correlation and facies variations for the Silurian formations from the Upper Yangtze Platform to the Lower Yangtze Platform, showing the interfingering of lithofacies and shoreline progradation with clastic dilution in the foredeep setting in the Lower Yangtze. The Lower Silurian Longmaxi equivalent strata include the Gaojiabian Formation in the Lower Yangtze. See inset map for location of the cross section.

Fig. 11. Jiaoye1 well, is the type well for the Upper Ordovician to Silurian shale in the Sichuan Basin, showing the facies, sequence stratigraphy, heterogeneity and shale reservoir characteristics. TST=transgressive systems tract, MFS=maximum flooding surface, HST=highstand systems tract, EHST=early HST, LHST=late HST. See Fig.1 for the location of the well. Well logs, TOC and gas content are from Guo (2013). Core photos are courtesy of Y. Ma with Sinopec in 2013.

Fig. 12. Structural traces indicating Caledonian, Indosinian, Yanshanian, and Himalayan tectonic events of different geologic ages. A, Yanchang Anticline, Zhenxiong, Yunnan; B, Luochang syncline, Gaoxian-Junlian, Sichuan; C, deformed syncline, Gulin, Sichuan; D, Longxiongchang syncline, Yibin-Zigong, Sichuan.

Fig. 13. Tectonic setting from the Sichuan Basin inside (Northern Zhaotong shale gas demonstration zone) to basin margin (SE Zhaotong shale gas demonstration zone) in the Upper Yangtze Platform.

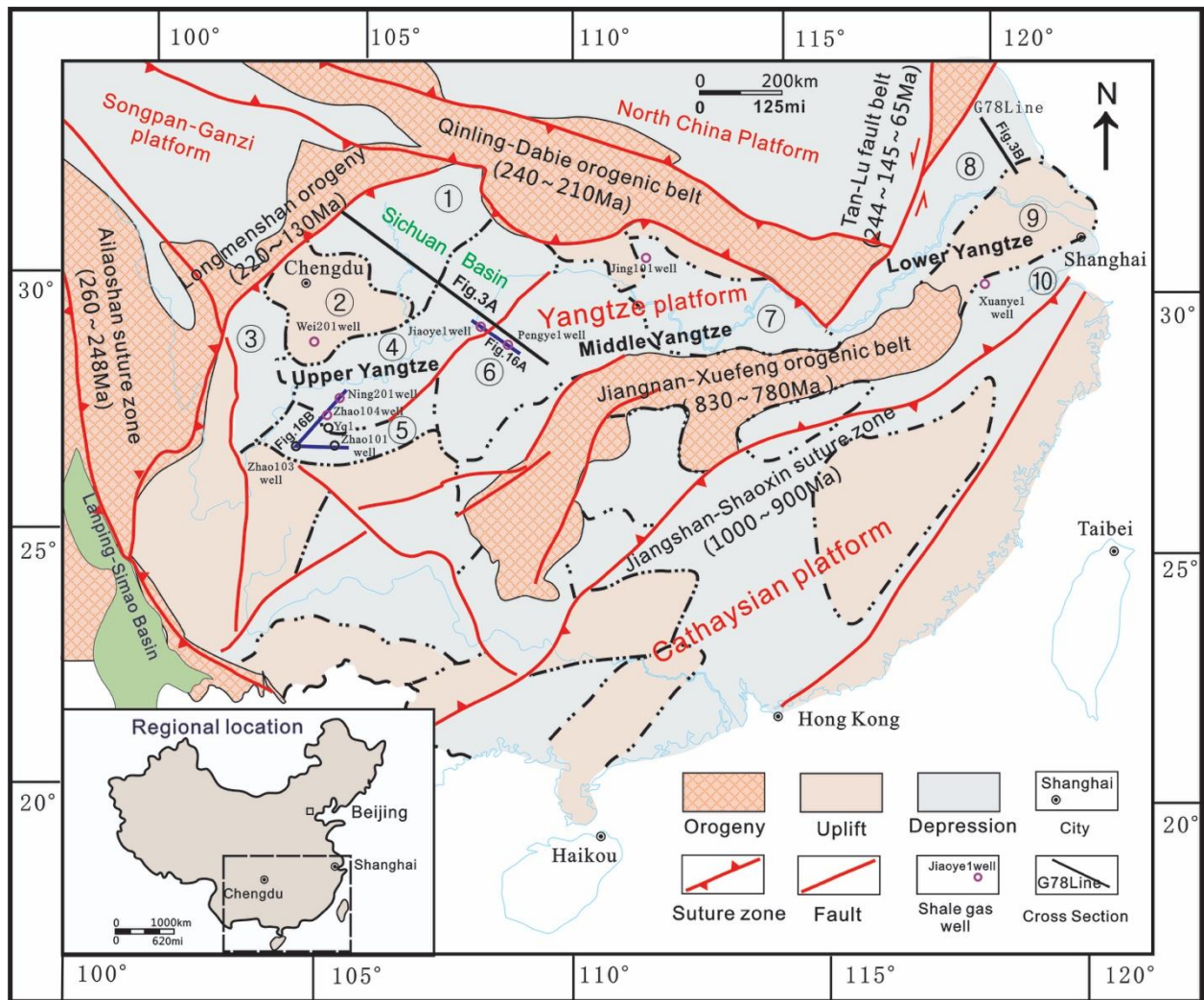
Fig. 14. Burial histories for representative wells in Upper, Middle and Lower Yangtze, showing tectonic activities and hydrocarbon generation history in different tectonic areas. A, Burial history of Dingshan1 well in Upper Yangtze; B, Burial history of Paishen1 well in Middle Yangtze; C, Burial history of Yan 1 well in Lower Yangtze; D, Index map for tectonic units and wells; cross-sections in Fig. 14 are also shown in red lines. Z=Pre-Cambrian Sinian, C=Cambrian, O=Ordovician, S=Silurian, D=Devonian, D1+2=Early and Middle Devonian, D3=Late Devonian, C=Carboniferous, P=Permian, J=Jurassic, K=Cretaceous, K3=Late Cretaceous, E=Paleogene, N=Neogene, Q=Quaternary. The well data of Paishen 1 and Yan 1 wells are from research report from Petroleum Exploration and Production Research Institute of Sinopec (H. Zheng, 2006). New age data and maturity data have been added for burial history and petroleum system simulation.

Fig. 15. Cross plot of the gas content and total organic content (TOC) for the Lower Cambrian Qiongzhusi shale and the Lower Silurian Longmaxi shale in the Yangtze Platform and comparison to typical U.S. marine shales. The data

from Jiaoye1 well is from Guo (2013) and the data for typical U.S. marine shales is from Hill and Nelson, 2000, Mavor, 2003 , and Jarvie, 2012.

Fig. 16. Schematic cross sections demonstrating the variations in formation pressure and initial shale gas production rates from the tectonically stable area inside the Sichuan Basin to the tectonically transitional area with tight synclines and many faults. A, Profile from the Jiaoye1 well in Jiaoshiba Shale Gas Field to the Pengye1 well in the Sanzheping syncline in Pengshui (modified from Guo, 2013). See Fig. 1 for location of the cross section; B, Profile from the Ning201 well in Changning pilot shale gas area to the Zhao101 well in the Zhaotong pilot shale gas area. See Fig. 1 for location of the cross section.

Fig. 17 Seismic reflection showing the complex tectonic setting in the Zhaotong shale gas demonstration zone outside the Sichuan Basin compared to the stable tectonic setting in the Changning shale gas demonstration zone inside the Sichuan Basin.



- ① Chuanbei depression ② Chuanzhong uplift ③ Chuanxinan depression ④ Chuandongnan depression
- ⑤ Dianqianbei depression ⑥ Xiang'E'xi depression ⑦ Hubei depression ⑧ Subei Depression
- ⑨ Sunan uplift ⑩ Qiantang depression

Fig.1

ACCEPTED MANUSCRIPT

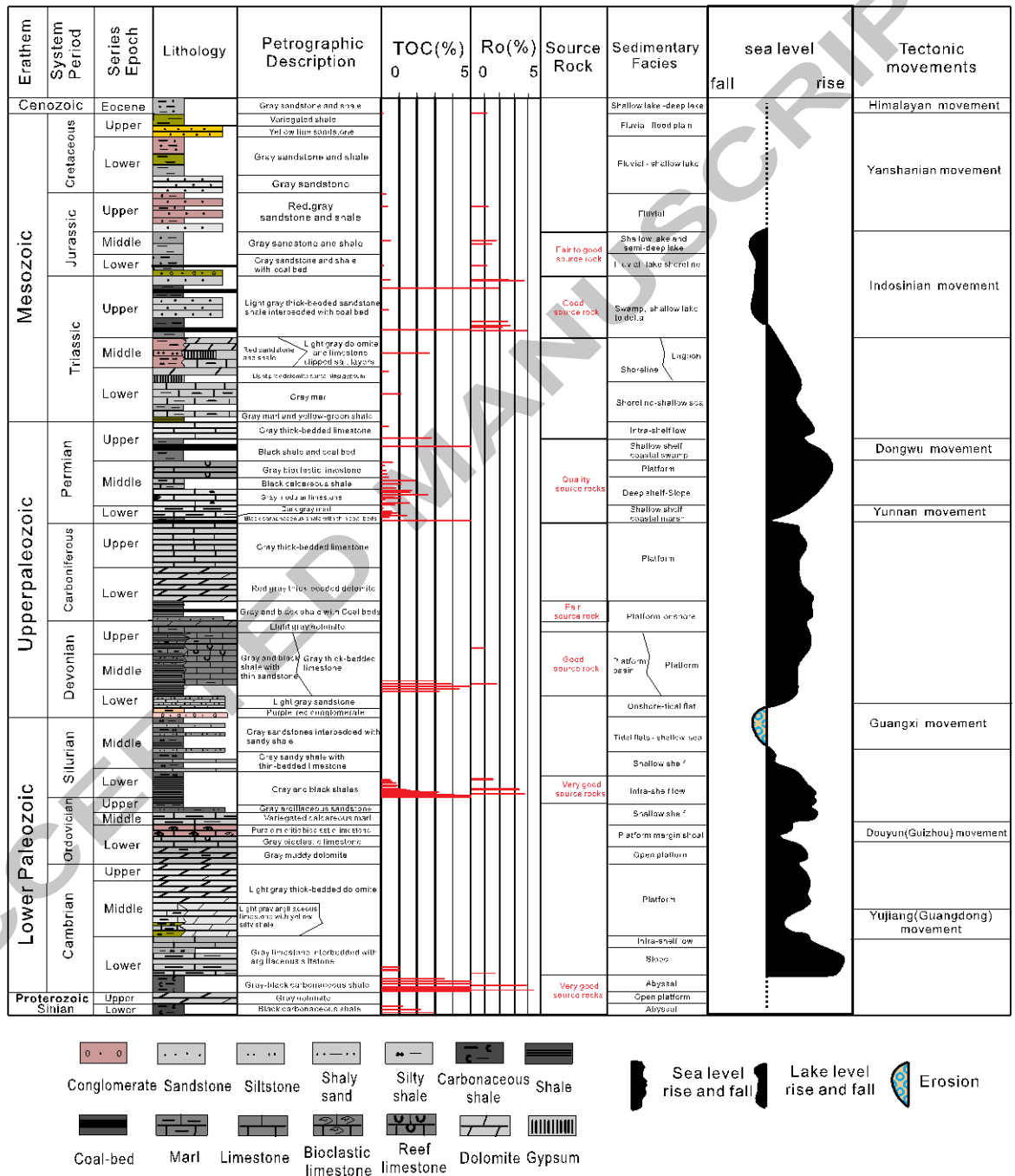


Fig. 2

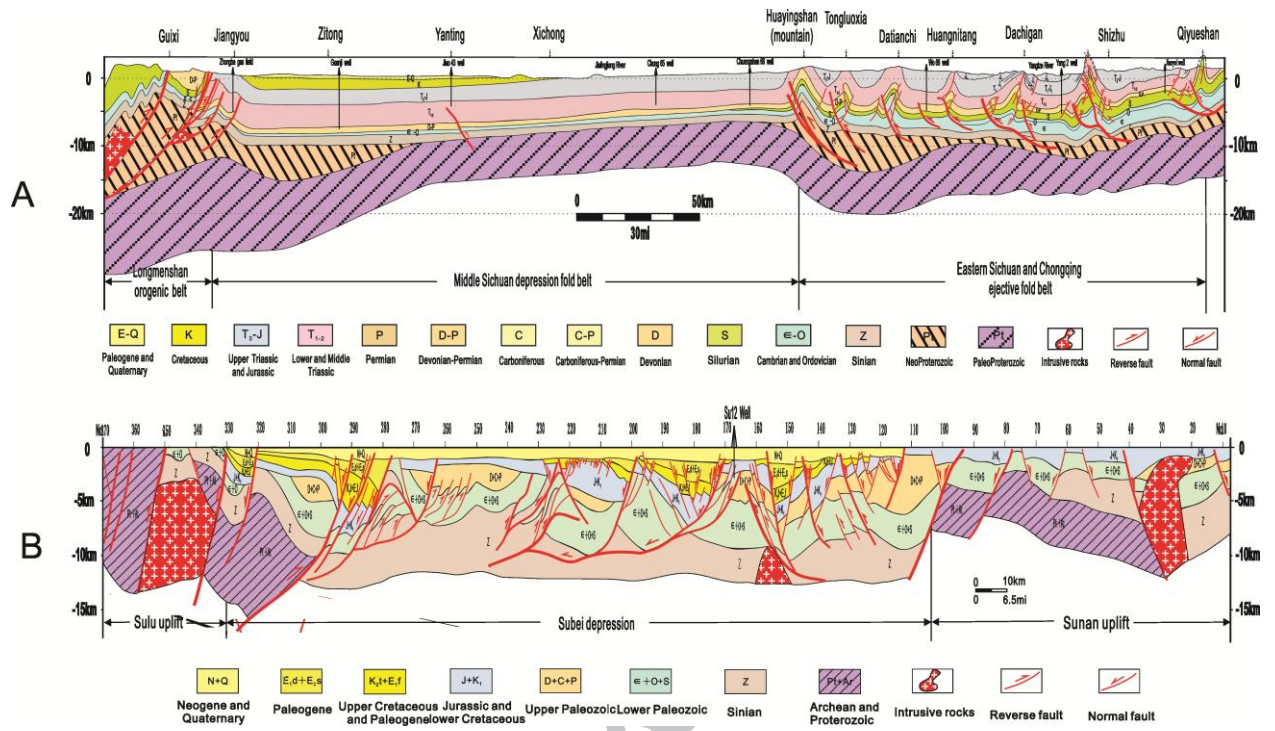


Fig. 3

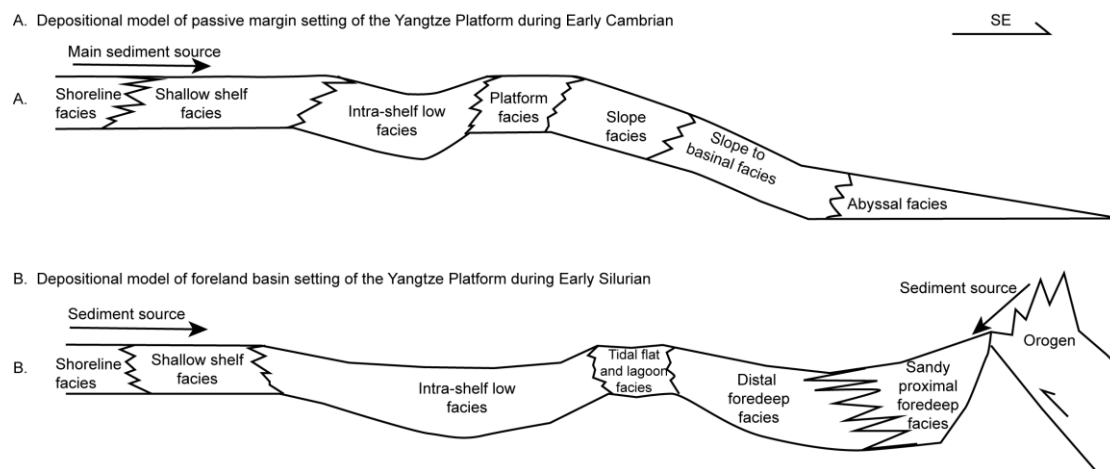


Fig. 4

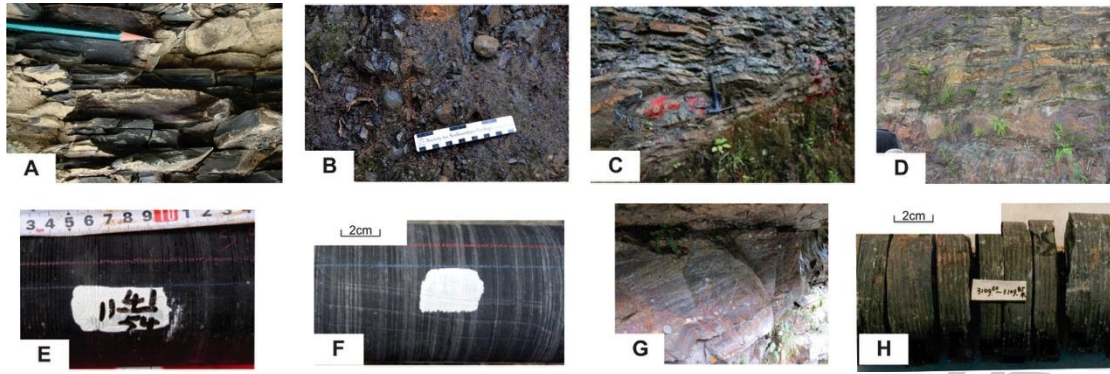


Fig. 5

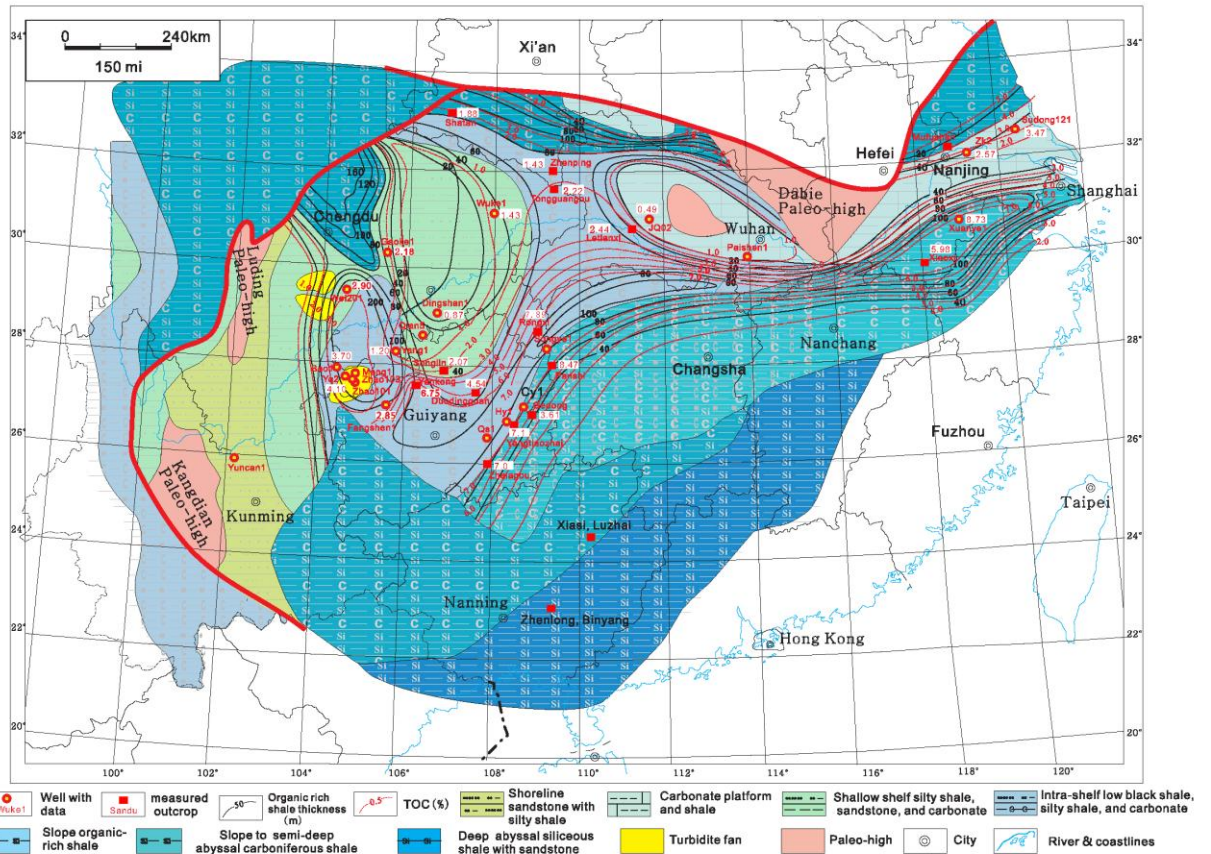


Fig. 6

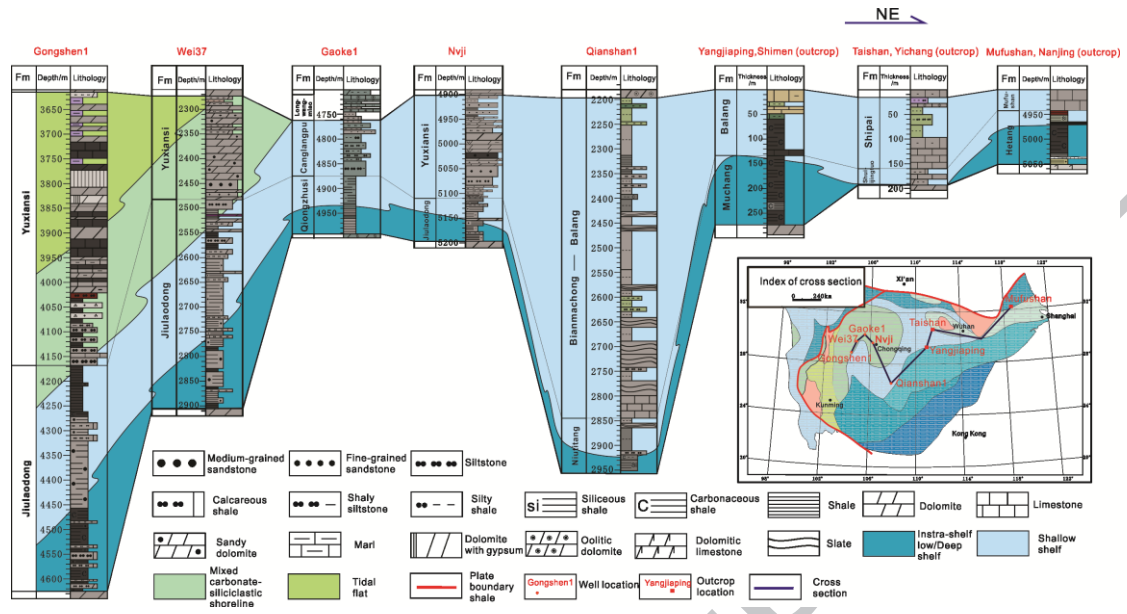


Fig. 7

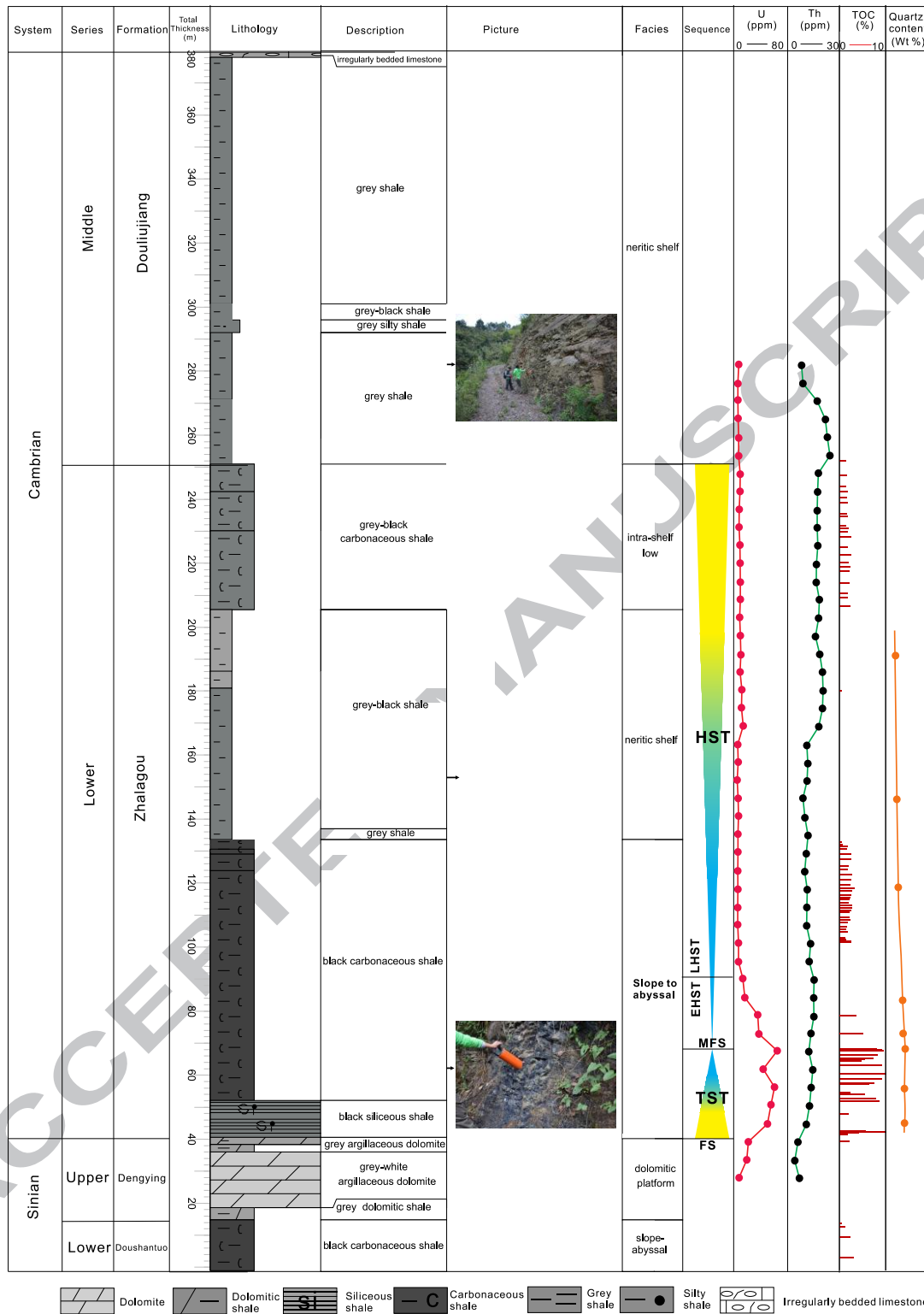


Fig. 8

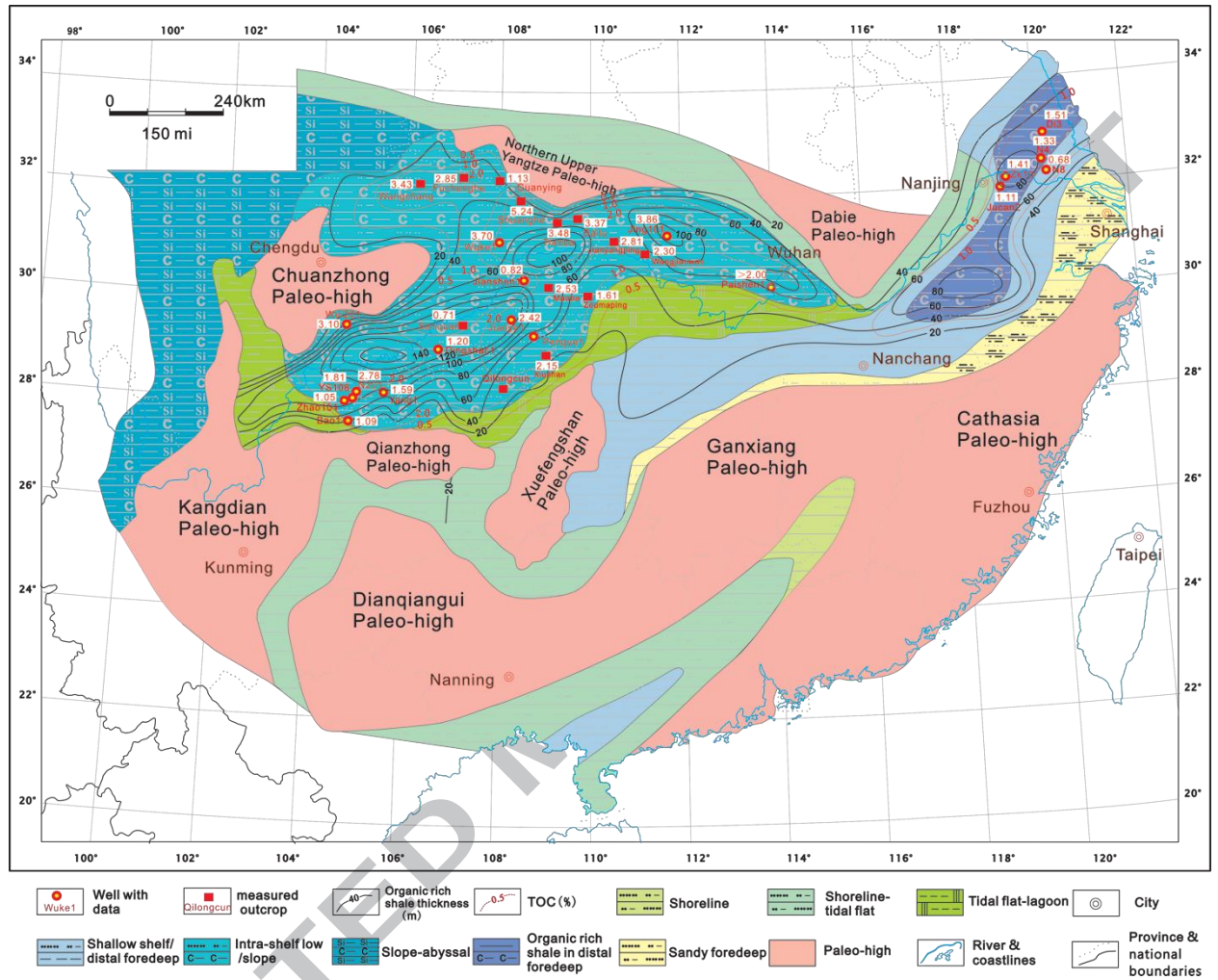


Fig. 9

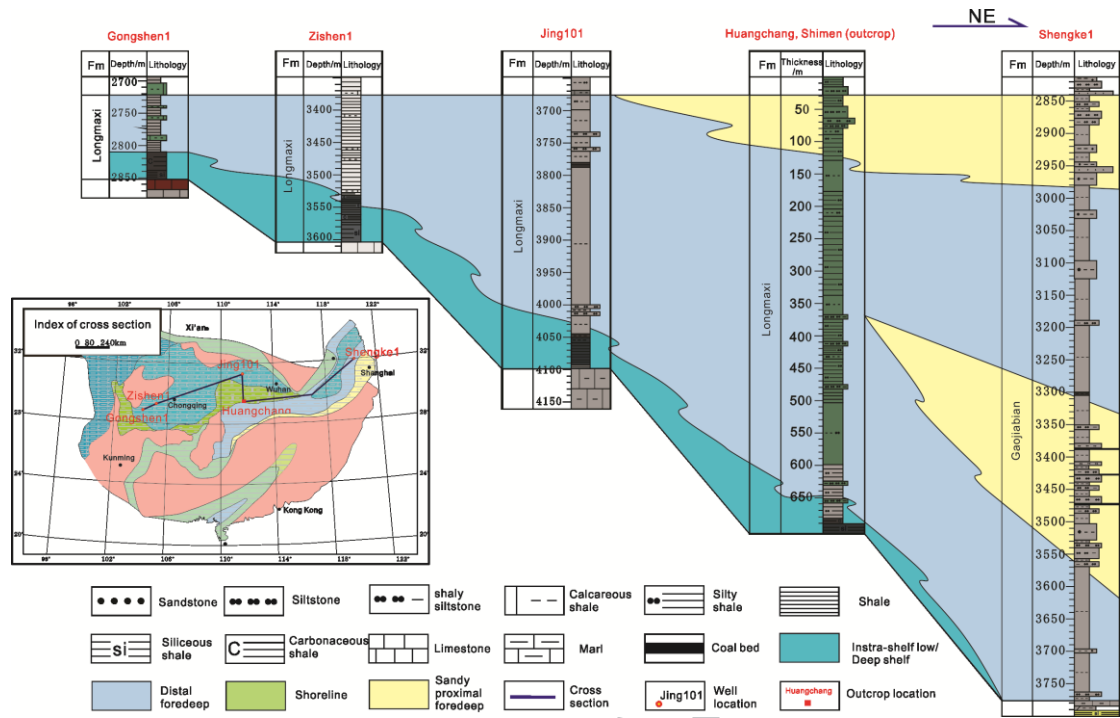


Fig. 10

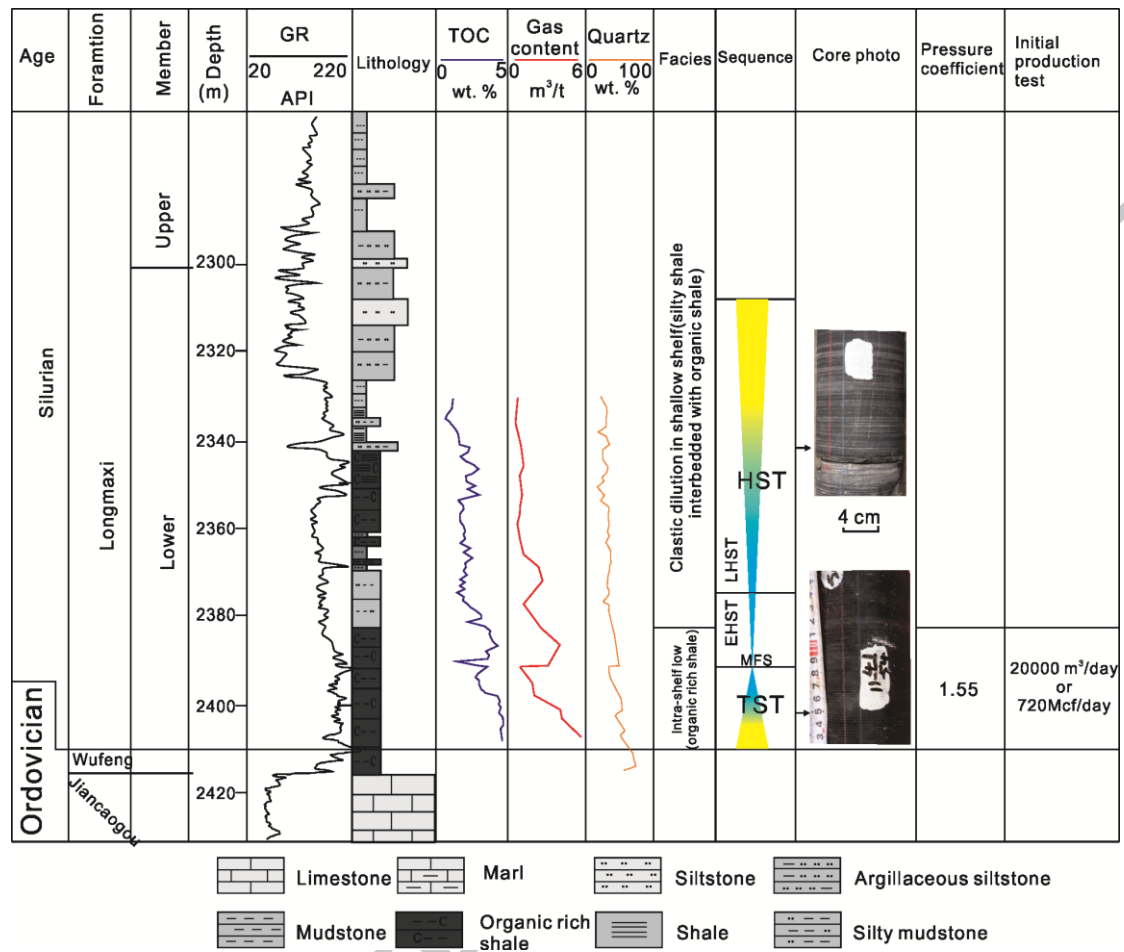


Fig. 11

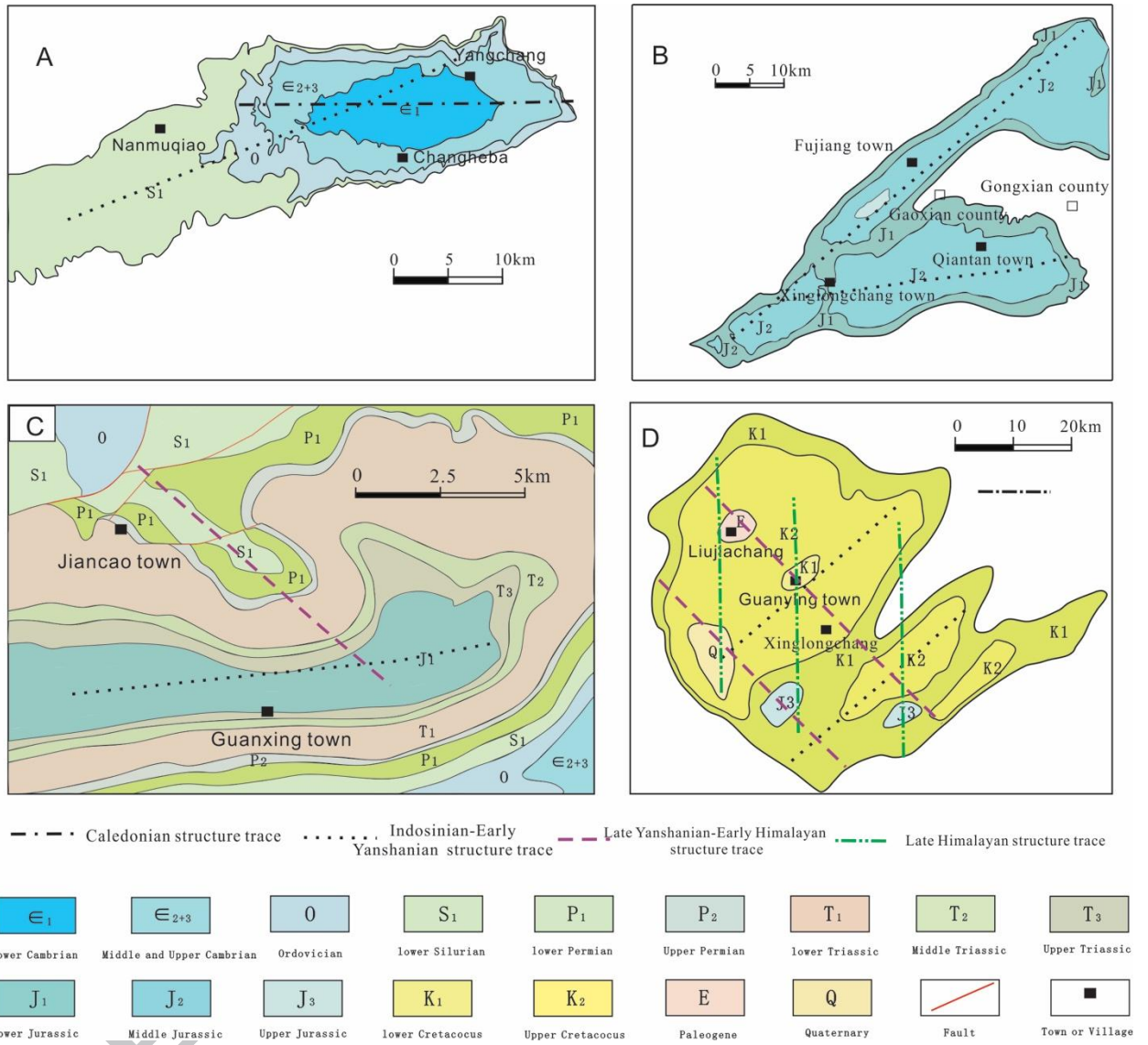


Fig. 12

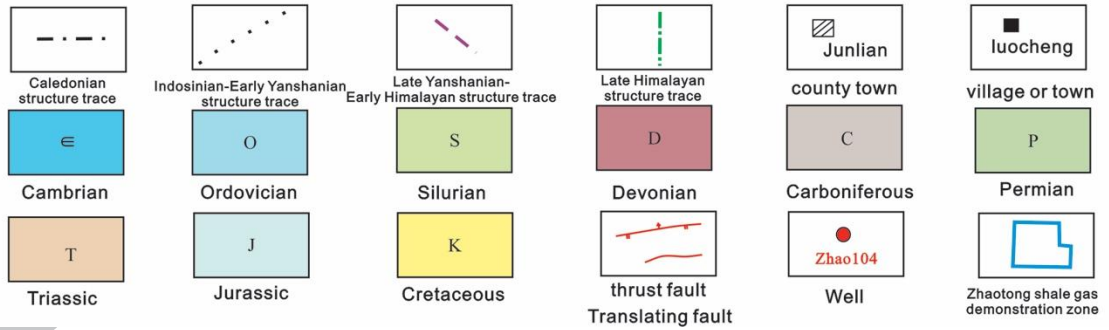
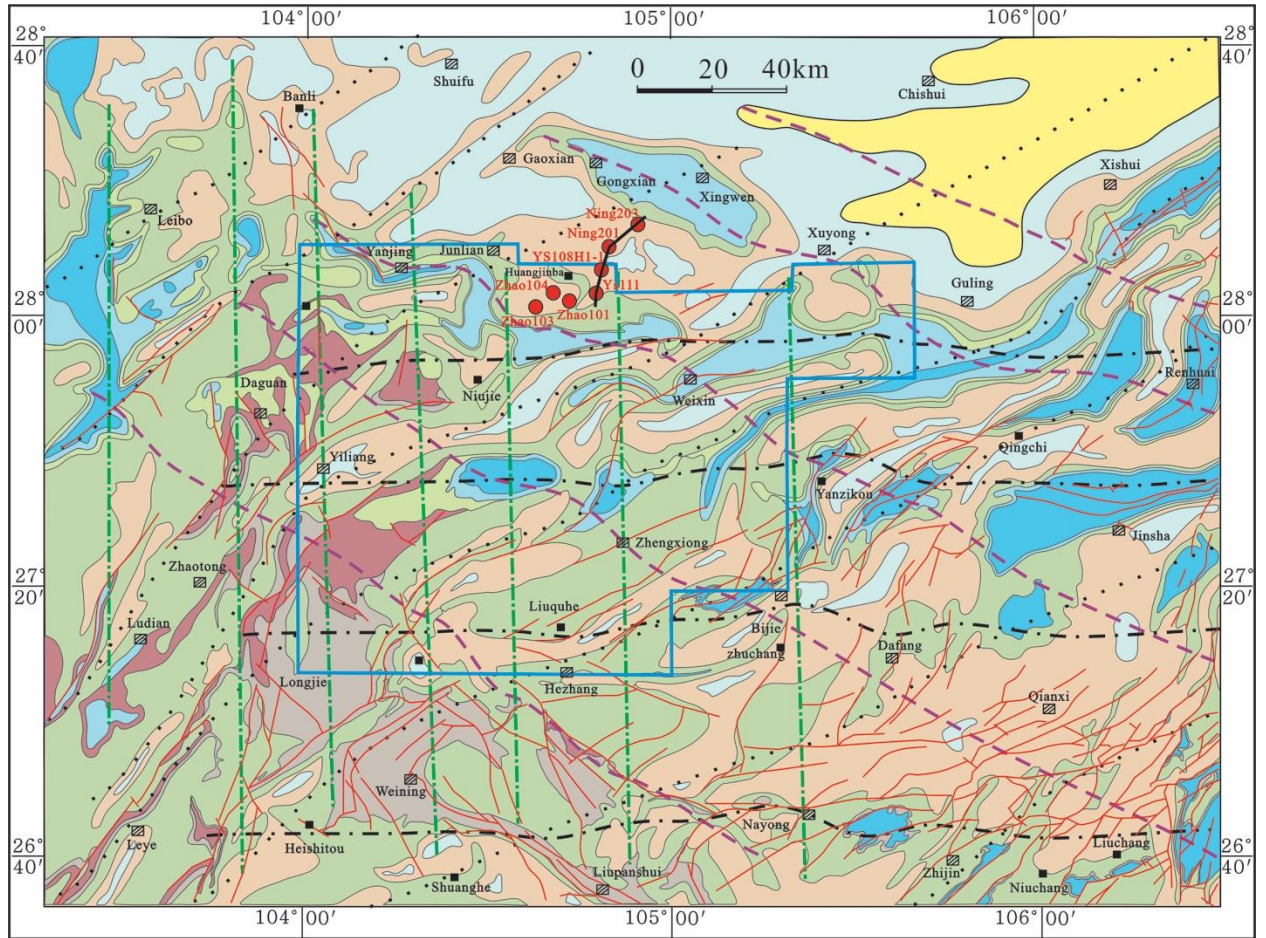


Fig. 13

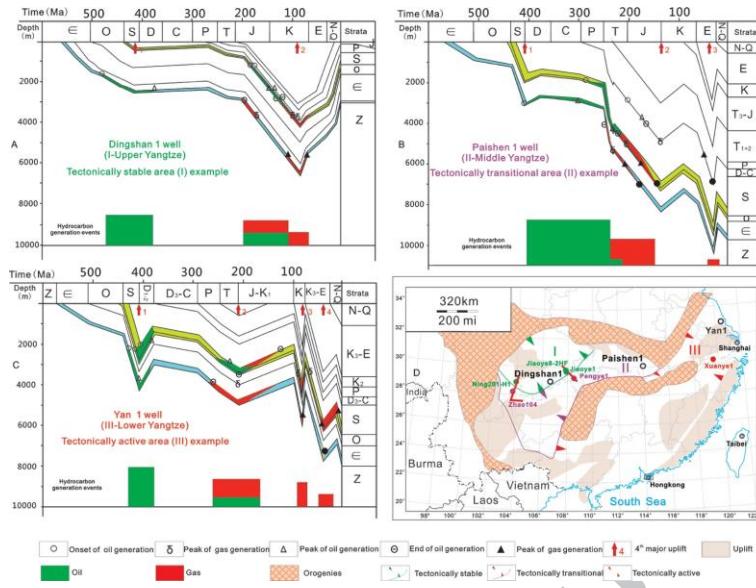


Fig. 14

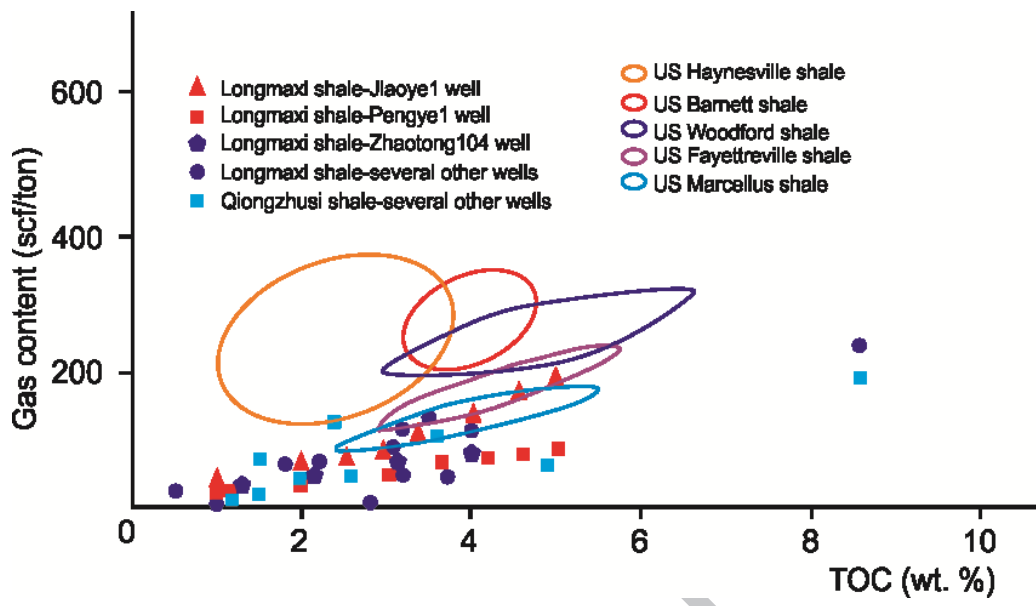


Fig. 15

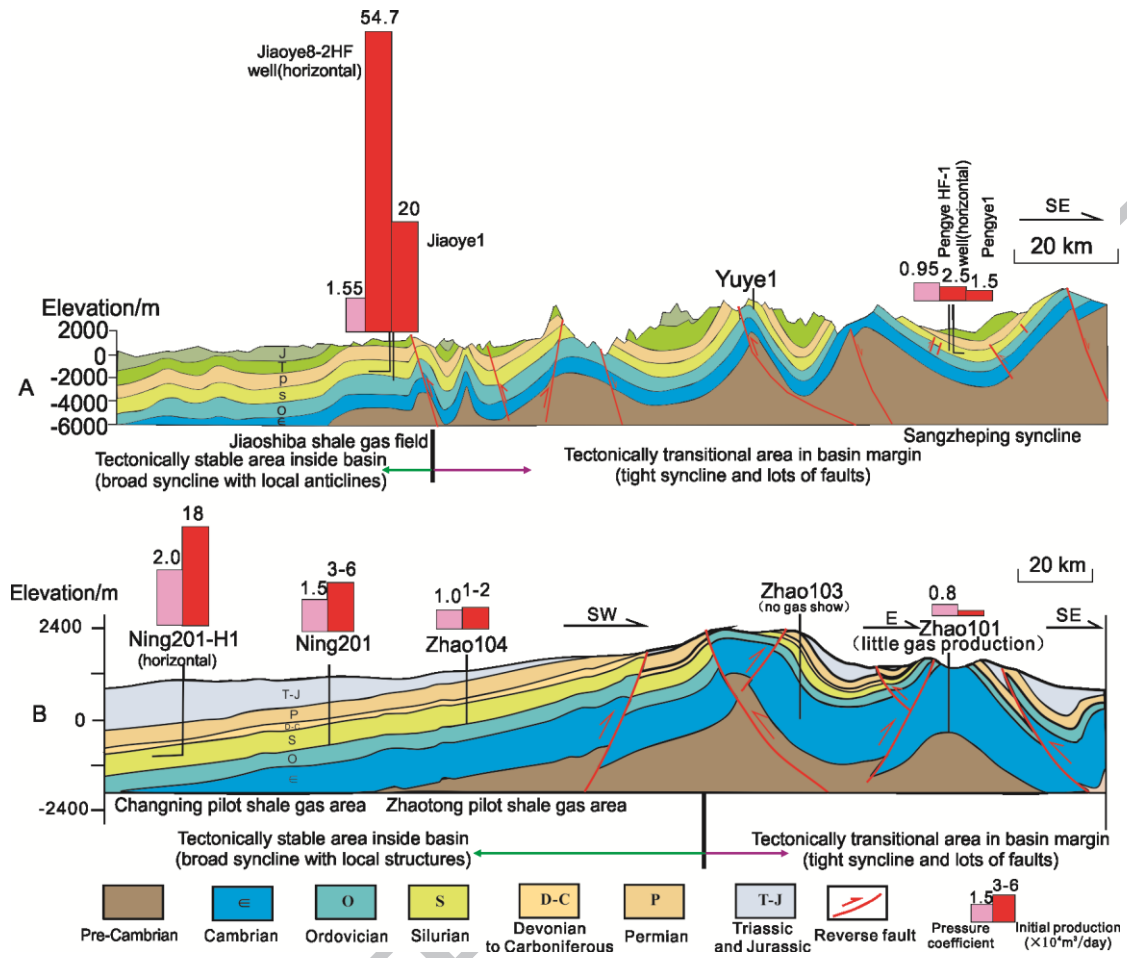


Fig. 16

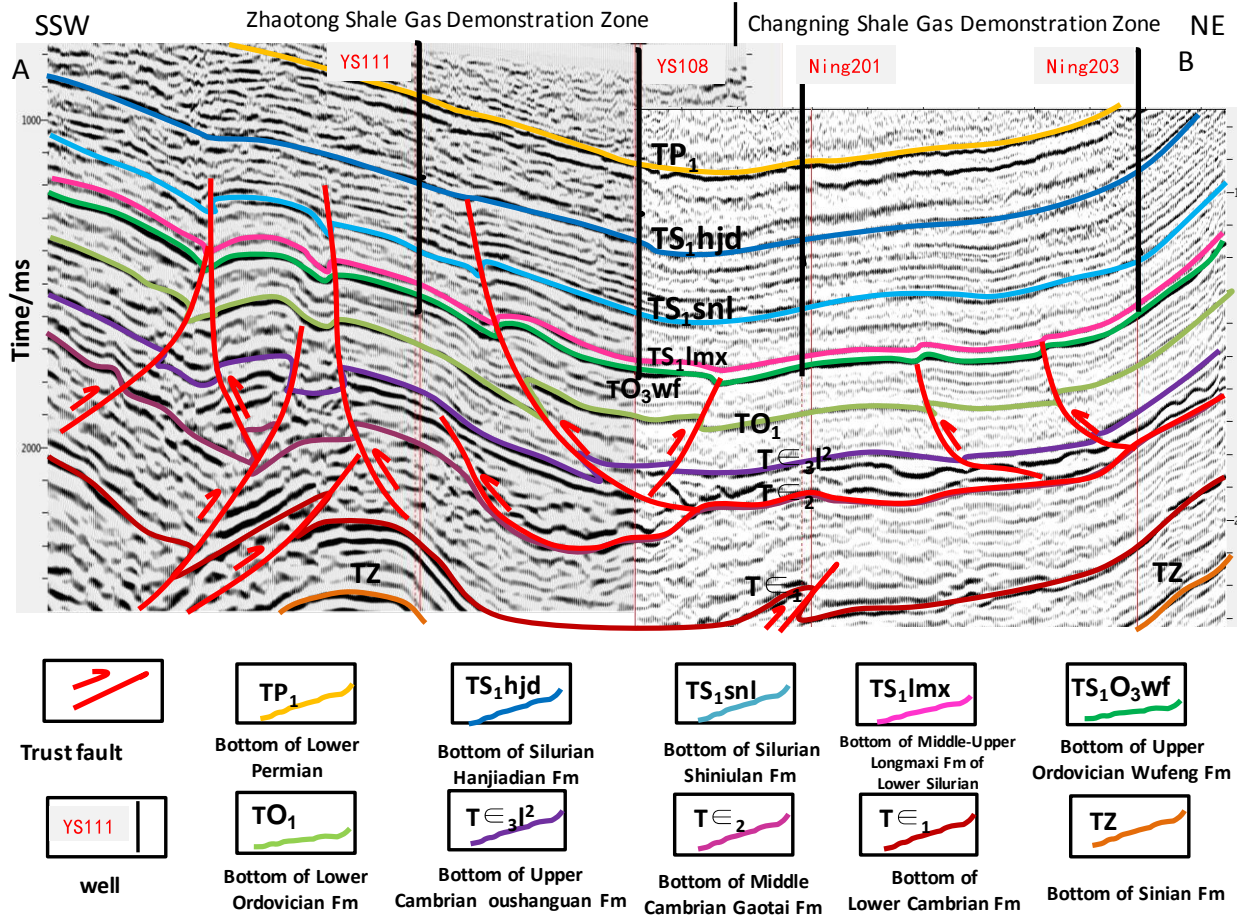


Fig. 17

Table 1

Bao1 (well)			Yangtiaoze (outcrop)			YQ2(well)			Zhalagou (outcrop)			Duodingguan (outcrop)			Yang1 (well)			Zhao103 (well)		
Depth/m	TOC /wt. %	Ro /%	Depth/m	TOC /wt. %	Ro /%	Depth/m	TOC /wt. %	Ro /%	Depth/m	TOC /wt. %	Ro /%	Depth/m	TOC /wt. %	Ro /%	Depth/m	TOC /wt. %	Ro /%	Depth/ m	TOC /wt. %	Ro /%
2719	0.36		115.12	2.09		48.25	0.80	4.01	73.83	0.20		337.83	1.49	2.89	2900.80	0.58	4.30	2433.45	1.02	
2728	0.46		114.00	2.62	2.00	59.42	0.82		211.02	0.13		327.75	1.93	3.11	2903.05	0.99	4.02	2499.32	1.63	
2734	0.5		110.33	6.80	2.86	77.11	1.12		537.26	0.75		325.61	2.47	3.13	2904.90	1.11	4.10	2501.32	1.30	2.14
2839		1.54	107.34	6.50	2.97	100.57	0.84	4.12	595.33	1.22	2.39	316.67	1.73	2.18	2905.90	1.23	3.99	2508.90	1.82	
2852	1.57		106.74	6.21	2.17	146.29	1.13		618.01	0.43		311.31	2.81	3.11	2906.75	1.23	4.25	2516.45	2.23	3.49
2878	1.68		100.63	7.63	3.34	157.59	0.94	4.06	625.20	0.95	2.43	277.97	2.21					2523.75	1.91	
2880.07		1.35	97.75	7.00	2.21	197.70	2.45		650.85	3.47	1.95	273.90	1.34	2.27				2659.38	2.23	
2891	1.28		68.19	2.41	2.87	218.80	2.71		659.44	6.00	2.78	271.93	1.71	3.11				2661.38	1.24	
2897		2.14	63.00	1.37	2.63	248.90	3.80		669.39	6.90	2.56	261.08	9.43	3.16				2662.68	1.38	3.75
2936	2.04		39.45	0.19		269.10	4.10		721.35	7.56	2.89	254.10	5.54	3.11						
2947	1.71		16.90	1.20		317.10	9.37		726.60	4.94		172.54	11.10	2.95						
2959	2.33	1.63	11.21	0.39		334.53	3.82					156.32	5.57	2.90						

Table 2

Bao1 (well)			Zhao104(well)		YS108(well)			Ning201 (well)			Wangjiawan (outcrop)			Jing101 (well)		
Depth/m	TOC/wt.%	Ro/%	Depth/m	TOC/wt.%	Depth/m	TOC/wt.%	Ro/%	Depth/m	TOC/wt.%	Ro/%	Depth/m	TOC/wt.%	Ro/%	Depth/m	TOC/wt.%	Ro/%
1176.00	8.58		1176.00	8.58	2382.38	0.51	1.59	2479.14	0.82	2.38	WL-1-19	2.83	1.30	4065.75	2.57	
1180.00	1.77	3.12	1180.00	1.77	2475.21	1.02	2.41	2485.35	0.50	2.41	WL-7-15	0.33	1.37	4070.10	2.84	2.96
1214.00	0.40	3.26	1185.00	4.54	2481.07	1.41	1.92	2491.35	1.28	2.47	WL-6-12	1.29		4073.66	4.20	3.28
1234.00	0.77	3.19	1214.00	0.40	2486.67	2.36	2.25	2495.30	2.43	2.48	WL-5-10	1.66		4076.05	3.78	2.82
1254.00	2.14	3.49	1234.00	0.77	2491.46	2.82	2.23	2501.44	2.76	2.56	WL-5-8	2.44		4079.81	3.39	4.05
1269.00	2.64		1248.00	1.65	2496.30	4.11	2.19	2504.62	4.76	2.64	WL-4-7	1.80		4086.26	4.80	2.87
1272.00	1.62	3.57	1251.00	1.96	2504.69	3.44	2.12	2510.89	2.61	2.69	WL-3-5	0.43		4090.14	4.52	2.98
1275.00	2.64		1259.00	2.09	2506.53	2.73	2.17	2514.00	3.62	2.71	WL-2-3	2.52	1.46	4093.00	5.98	2.75
1279.00	1.85	3.52	1261.00	2.17	2510.65	3.54	2.30	2521.27	1.64	2.83				4095.10	5.15	2.82

Table 3

Depth(m)	TOC(%)	Gas content (m ³ /t)	Quartz content(%)	Clay content(%)
2330.35	1.02	0.66	26.83	61.45
2342.66	2.11	0.88	28.05	55.42
2363.44	1.57	0.95	29.27	32.53
2366.81	2.47	1.17	37.80	38.55
2369.71	1.81	2.34	30.49	42.17
2383.53	1.50	2.41	36.59	38.55
2387.59		4.02	46.34	34.94
2391.89	3.25	2.56	35.37	42.17
2395.25	2.82		40.24	34.94
2397.00	3.00	1.02	42.68	36.14
2401.29	4.20		51.22	26.51
2402.45		4.10	42.68	19.28
2405.24	4.52		48.78	30.12
2412.32		4.17	56.10	21.69
2414.18	4.40		54.88	36.14

Table 4

Area Parameter	Zhaotong-Huangjinba (outside basin)	Changning (inside basin)	Weiyuan (inside basin)	Jiaoshiba/Fuling (inside basin)
Structure	Complex syncline with southern limb deformed	Complex syncline with gentle northern limb	Limb of paleo-high	Box shaped anticline in gentle syncline
Stress	shear + compression	Compressional-shear	Compressional-shear	Mainly compression
Vertical Depth, m	2530	2650	3897	2500
Thickness, m	31~35	30~46	24~40	30~40
TOC, %	2.1~6.7	2.8~5.3	2.2~3.3	2~6
Porosity, %	2.0~5.0	2.9~5.0	2.4~4.87	4~6
Total gas content, m ³ /t	1.5~3.5	1.7~3.5	2.5~4.35	4.7~5.7
Pressure Coefficient	1~1.96/5 wells (in syncline axis)	1.30~2.02/4 wells	1.40~1.96/54 wells	1.55/134 wells
Clay content, %	27.5	25.2	31~45	30
Horizontal stress contrast, MPa	20~30	10~13	15~9	3~6
Young's modulus, MPa	35000	33940	19930	35000
Poisson's ratio	0.20	0.21	0.18	0.21
Brittle index	47~65	55~65	46~69	50~65
Fracture development	Abundant	Local development	Local development	Many fractures

Highlights

- Tectonics and depositional settings of Lower Paleozoic marine shales on the Yangtze Platform are revealed.
- Relationship between tectonics, facies and shale gas accumulation are deciphered.
- Stable tectonics and siliceous organic-rich facies are favorable for shale gas exploration and production.